Nuclear Reactor Laboratory
UWNR University of Wisconsin-Madison
1513 University Avenue, Room 1215 ME, Madison, WI 53706-1687, Tel: (608) 262-3392, FAX: (608) 262-8590
email: reactor@engr.wisc.edu, http://reactor.engr.wisc.edu

June 21, 2010 RSC 1051

United States Nuclear Regulatory Commission
ATTN: Document Control Desk
Washington, D.C. 20555

Subject: Docket 50-156, License R-74
Reactor Start-Up Report following Order to Convert from High to Low Enriched Uranium Fuel at the University Of Wisconsin Nuclear Reactor
TAC No. MD9592 (EA-09-141)

Dear Sirs:

By Order, dated June 11, 2009, the Commission modified facility operating license R-74 for the purpose of conversion of the reactor from high to low enriched uranium fuel. In accordance with that order a reactor start-up report is required to be submitted to the NRC within 6 months following the return to normal reactor operations.

Normal reactor operations resumed on January 22, 2010 following extensive physics testing of the reactor. Enclosed you will find a report detailing the results of this testing. This report follows the suggested format for reactor startup reports found in attachment 3 to the above reference order, EA-09-141.

Sincerely,

Robert J. Agasie
Reactor Director

Enclosure

A020
NRR

THE UNIVERSITY OF WISCONSIN
NUCLEAR REACTOR LABORATORY

REACTOR START-UP REPORT

Prepared to meet reporting requirements of:

U. S. Nuclear Regulatory Commission

Order to Convert from

High to Low Enriched Uranium Fuel

at the

University Of Wisconsin Nuclear Reactor

License R-74

June 21, 2010

THE UNIVERSITY of WISCONSIN
MADISON

Table of Contents

A. HISTORICAL BACKGROUND 3
B. DISPOSITION OF OLD TRIGA FUEL 3
C. APPROACH TO CRITICAL EXPERIMENT 4
D. LOADING TO J21-R0 CORE 12
E. LOADING TO J21-R14 OPERATIONAL CORE 19
F. OPERATIONAL CORE REACTIVITY MEASUREMENTS 29
F.1 REFLECTOR REACTIVITIES (REFLECTED) 29
F.2 COOLANT VOID COEFFICIENT 30
F.3 EXPERIMENTAL FACILITY REACTIVITY MEASUREMENTS 32
G. POWER CALIBRATIONS 34
H. POWER DEFECT MEASUREMENTS 35
I. FUEL TEMPERATURE MAPPING 40
J. FLUX MEASUREMENTS 44
K. PULSE TESTING 46
L. SQUARE-WAVE TESTING 52
M. SUMMARY OF HEU MEASUREMENTS VS. LEU PREDICTIONS AND MEASUREMENTS 54
N. COMPUTING MCNP MODEL BIAS 58

A. HISTORICAL BACKGROUND

The University of Wisconsin Nuclear Reactor achieved initial criticality on March 26, 1961 as an MTR-type flat-plate core. It was operated at a licensed maximum power level of 10 kW, with an upgrade to 250 kW on October 22, 1964. The MTR core was replaced with a Standard TRIGA core achieving first criticality on November 14, 1967 with a licensed nominal power of 1.0 MW. MTR fuel was shipped off-site in 1986. The Standard TRIGA core was shutdown on March 1, 1974 after a total exposure of 145.0 MWd.

The Standard TRIGA core was converted in multiple phases to an all TRIGA FLIP (Fuel Life Improvement Plan) HEU core. The first mixed core with 9 FLIP bundles achieved criticality on March 12, 1974, the second mixed core with 15 FLIP bundles on January 3, 1978, and the final all FLIP core on June 15, 1979. The all FLIP core was shutdown on August 19, 2009 after a total exposure of 843.5 MWd and 1074.7 critical days. This includes the exposure of the Standard TRIGA core and mixed cores. The exposure of individual FLIP bundles ranged from 629.3 to 698.5 MWd.

B. DISPOSITION OF OLD TRIGA FUEL

During conversion to TRIGA FLIP fuel, the Standard TRIGA fuel was unloaded from the core into the fuel storage pit. This Standard TRIGA fuel remained in the storage pit throughout almost the entire FLIP core history, leaving just enough room to unload the FLIP operational core if needed. In order to convert to TRIGA LEU 30/20 fuel, the Standard TRIGA fuel had to be shipped off-site to make room in the fuel storage pit. In May 2009, 120 Standard TRIGA fuel elements were shipped to Idaho National Laboratory, leaving 8 Standard TRIGA fuel elements remaining. After the FLIP core was shutdown, it was unloaded into the fuel storage pit, as were the lightly-irradiated FLIP fuel elements which had been stored in the fresh fuel vault. All TRIGA Standard and FLIP fuel elements (8 Standard and 101 FLIP) are currently being stored in the fuel storage pit awaiting shipment to Idaho National Laboratory sometime in 2010.

C. APPROACH TO CRITICAL EXPERIMENT

TRIGA LEU 30/20 fuel loading began on September 8, 2009. Fuel bundles were loaded based on 1/M plot predictions to the locations indicated in Figure 1 following procedure UWNR 143, which complies with standard ANS-1. The complete fuel loading sequence is included in Table 1. Subcritical multiplication data is shown in Table 2 and inverse count rate ration (1/M) data in Table 3. Figure 2 through Figure 4 represent the 1/M plots for the varying core geometries. In the figures, FC is the installed Fission Counter, and AFC is the Auxiliary Fission Counter. Initial criticality was achieved on September 16, 2009 at 14:32 with core loading J18-R0 (18 fuel bundles, 0 reflectors). The critical bank height was 17 inches (full out on all control elements except the transient rod), and the excess reactivity was estimated as 0.074 %Δk/k by withdrawing the transient rod full out to 19.71 inches and measuring the doubling time. The shutdown margin with the most reactive control blade and non-scrammable control blade withdrawn, hereafter called the technical specification shutdown margin, was measured to be 5.26 %Δk/k, which satisfied the acceptance criteria of 0.2 %Δk/k.

Table 1, Fuel Loading Sequence

Date	Time	Item	To
9/8/2009	13:47	Bundle 61	D5 (SE)
9/9/2009	10:45	Install t-rod and drive	
9/10/2009	14:20	Bundle 62	D4 (SW)
9/10/2009	14:25	IFE 11749	D4 (SW)
9/10/2009	14:37	Bundle 63	D6
9/10/2009	14:40	Bundle 64	E5
9/10/2009	14:43	Bundle 65	C5
9/11/2009	12:39	Bundle 66	E6
9/11/2009	12:41	Bundle 67	C4
9/14/2009	11:06	Bundle 68	E4
9/14/2009	11:08	Bundle 69	C6
9/14/2009	14:13	Bundle 70	C3
9/15/2009	08:41	Bundle 71	E7
9/15/2009	11:12	Bundle 72	E3 (NE)
9/15/2009	11:16	IFE 11748	E3 (NE)
9/15/2009	11:31	Bundle 73	C7
9/15/2009	11:34	Bundle 74	F6
9/16/2009	07:53	Bundle 75	B4
9/16/2009	09:33	Bundle 76	F4
9/16/2009	11:06	Bundle 77	B6
9/16/2009	13:08	Bundle 78	B3
9/21/2009	09:31	Bundle 79	F7
9/21/2009	13:24	Bundle 80	F3
9/22/2009	09:55	Bundle 81	B7

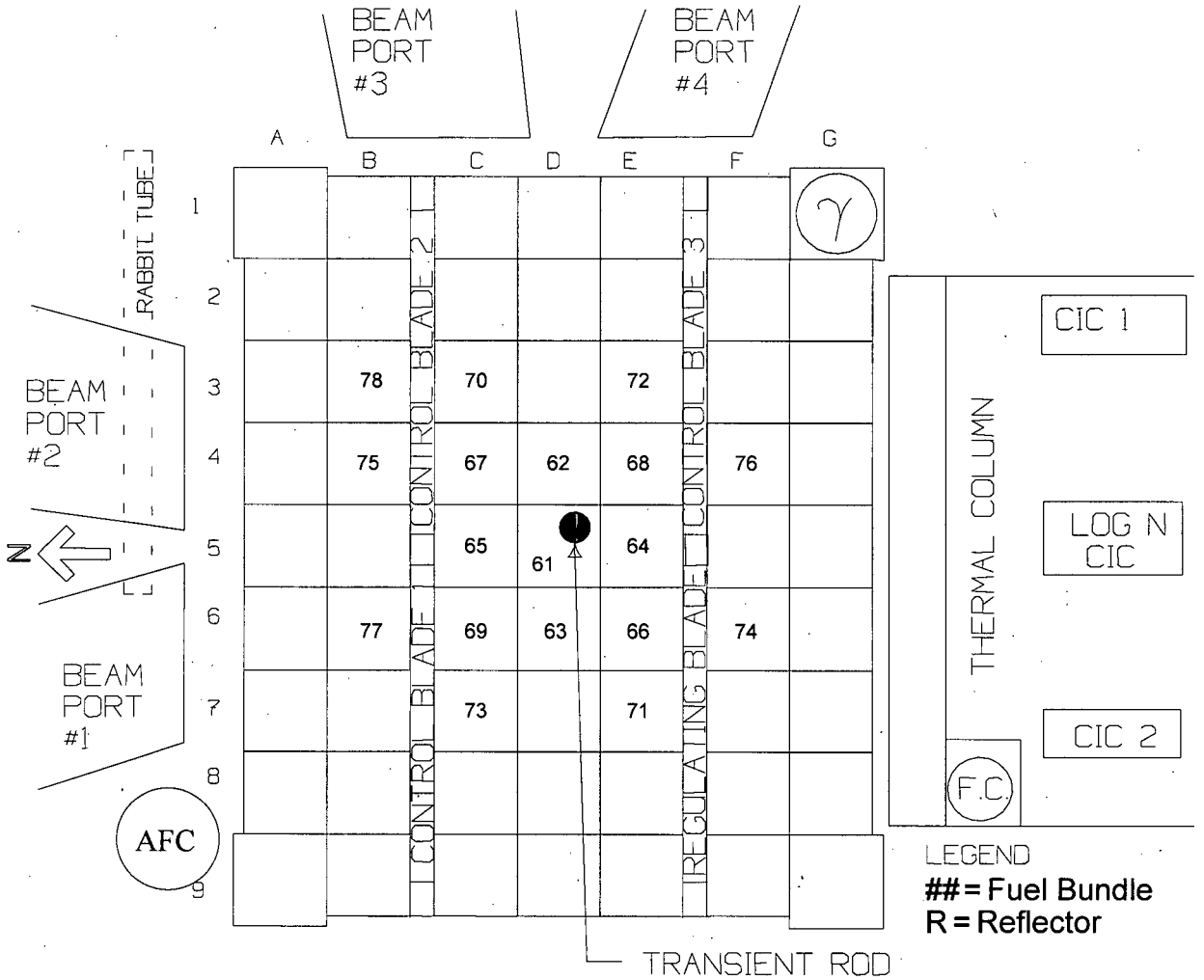

Figure 1, J18-R0 Initial Critical Core Map

Table 2, Measured 1/M Count Data (no reflectors installed)

Bundle Added	Total	Bank full in			Bank half out			Bank full out		
		FC	AFC	Min	FC	AFC	Min	FC	AFC	Min
D5	1	26734*	5296	240	14867	2676	160	16773	3138	180
D4	2	N/A	N/A	N/A	N/A	N/A	N/A	N/A	N/A	N/A
D6	3									
E5	4									
C5	5	24241	6644	240	11983	3651	120	12010	3882	120
E6	6	N/A	N/A	N/A	N/A	N/A	N/A	N/A	N/A	N/A
C4	7	7766	2528	75	7887	2961	75	7669	3530	75
E4	8	N/A	N/A	N/A	N/A	N/A	N/A	N/A	N/A	N/A
C6	9	6237	3095	60	6607	4248	60	3914	3039	30
C3	10	5045	3011	45	3482	2764	30	4189	4149	30
E7	11	5320	3192	45	3707	3130	30	4674	4586	30
E3	12	N/A	N/A	N/A	N/A	N/A	N/A	N/A	N/A	N/A
C7	13									
F6	14	6027	4599	30	3827	4195	15	7375	9202	15
B4	15	6377	5599	30	4048	5492	15	9331	15189	15
F4	16	4290	3061	15	4213	4556	10	15971	19670	10
B6	17	2856	3643	10	4599	10804	10	17610	53372	4
B3	18	2974	4027	10	2992	7589	6	Critical		

* 5 bundle count data was used as R_0 for FC Bank full in; suspect 1 bundle R_0 count is corrupted.

Table 3, Calculated 1/M Values (no reflectors installed)

Total Bundles	Bank full in		Bank half out		Bank full out	
	1/M FC	1/M AFC	1/M FC	1/M AFC	1/M FC	1/M AFC
1	1.000	1.000	1.000	1.000	1.000	1.000
2	N/A	N/A	N/A	N/A	N/A	N/A
3						
4						
5	1.000*	0.797	0.931	0.550	0.931	0.539
6	N/A	N/A	N/A	N/A	N/A	N/A
7	0.975	0.655	0.884	0.424	0.911	0.370
8	N/A	N/A	N/A	N/A	N/A	N/A
9	0.972	0.428	0.844	0.236	0.714	0.172
10	0.901	0.330	0.801	0.182	0.667	0.126
11	0.854	0.311	0.752	0.160	0.598	0.114
12	N/A	N/A	N/A	N/A	N/A	N/A
13						
14	0.503	0.144	0.364	0.060	0.190	0.028
15	0.475	0.118	0.344	0.046	0.150	0.017
16	0.353	0.108	0.221	0.037	0.058	0.009
17	0.354	0.061	0.202	0.015	0.021	0.001
18	0.340	0.055	0.186	0.013	Critical	

* 5 bundle count data was used as R_0 for FC Bank full in; suspect 1 bundle R_0 count is corrupted.

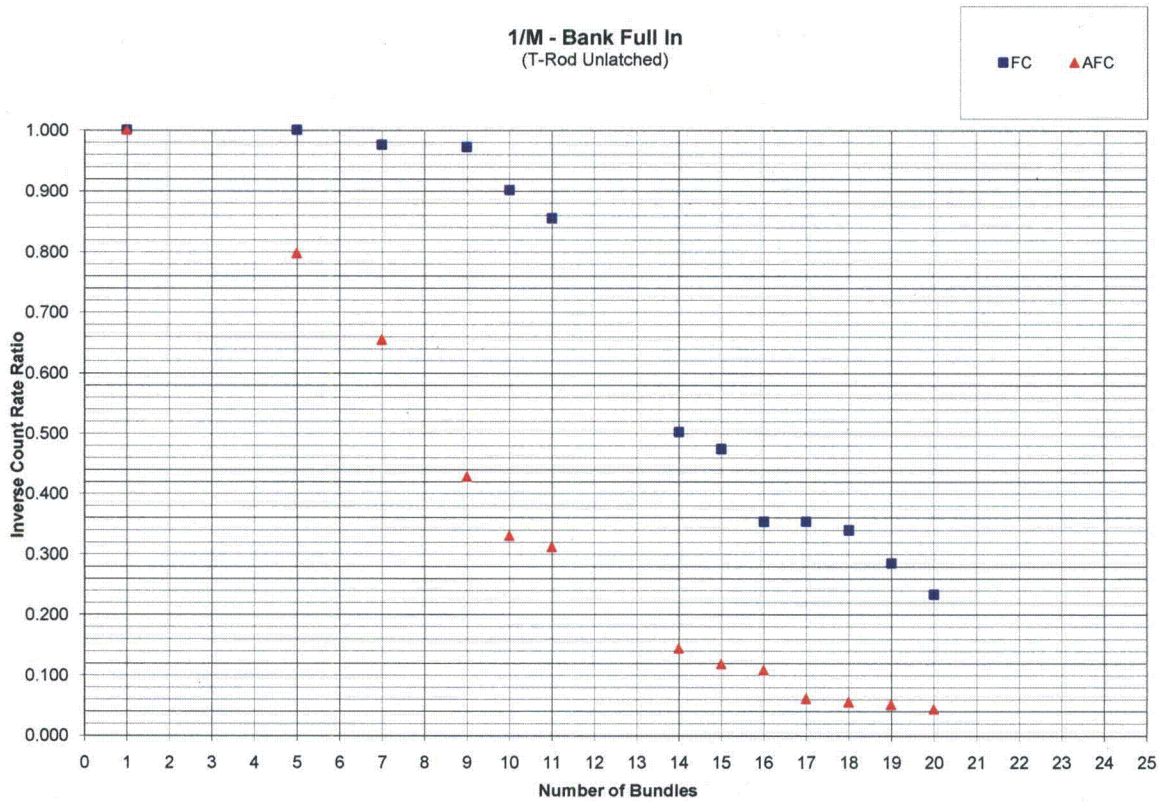

Figure 2, Bank Full In 1/M Plot

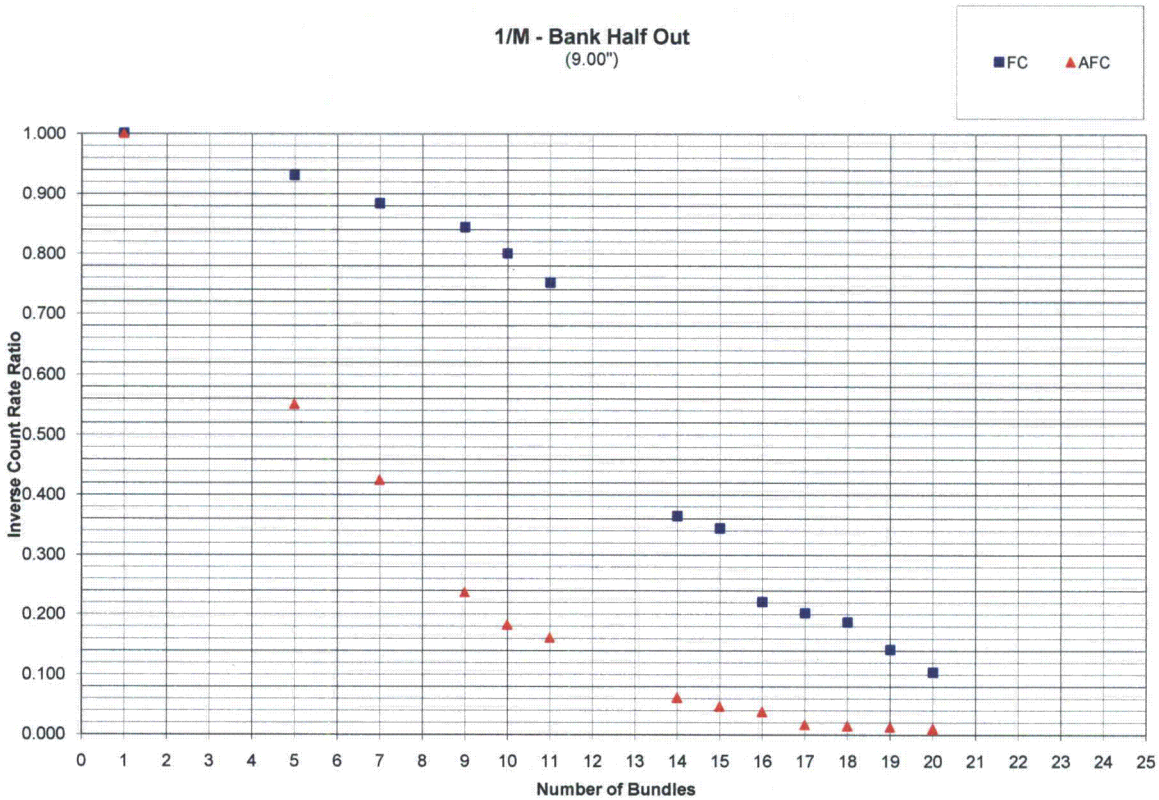

Figure 3, Bank Half Out 1/M Plot

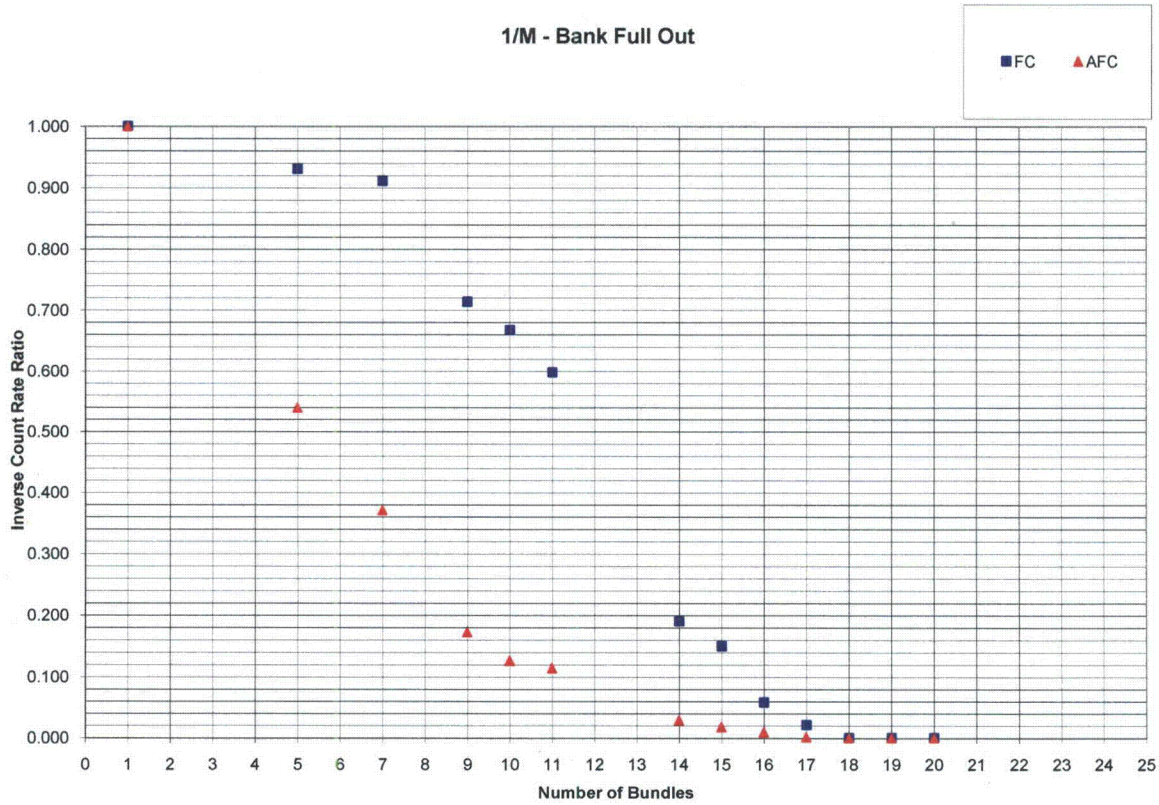

Figure 4, Bank Full Out 1/M Plot

The measured critical configuration is compared to the LEU conversion analysis prediction in Table 4.

Table 4, Predicted vs. Measured Critical Configuration

	LEU Predicted	LEU Measured
Critical bundles	19	18

D. LOADING TO J21-R0 CORE

Fuel loading continued utilizing inverse multiplication plots to assure each subsequent fuel bundle could be loaded safely. After each fuel addition absolute and technical specification shutdown margin measurements were made. The final unreflected 21 bundle core is shown in Figure 5. The subcritical count rate data and 1/M plot predictions are shown in Table 5 and Table 6.

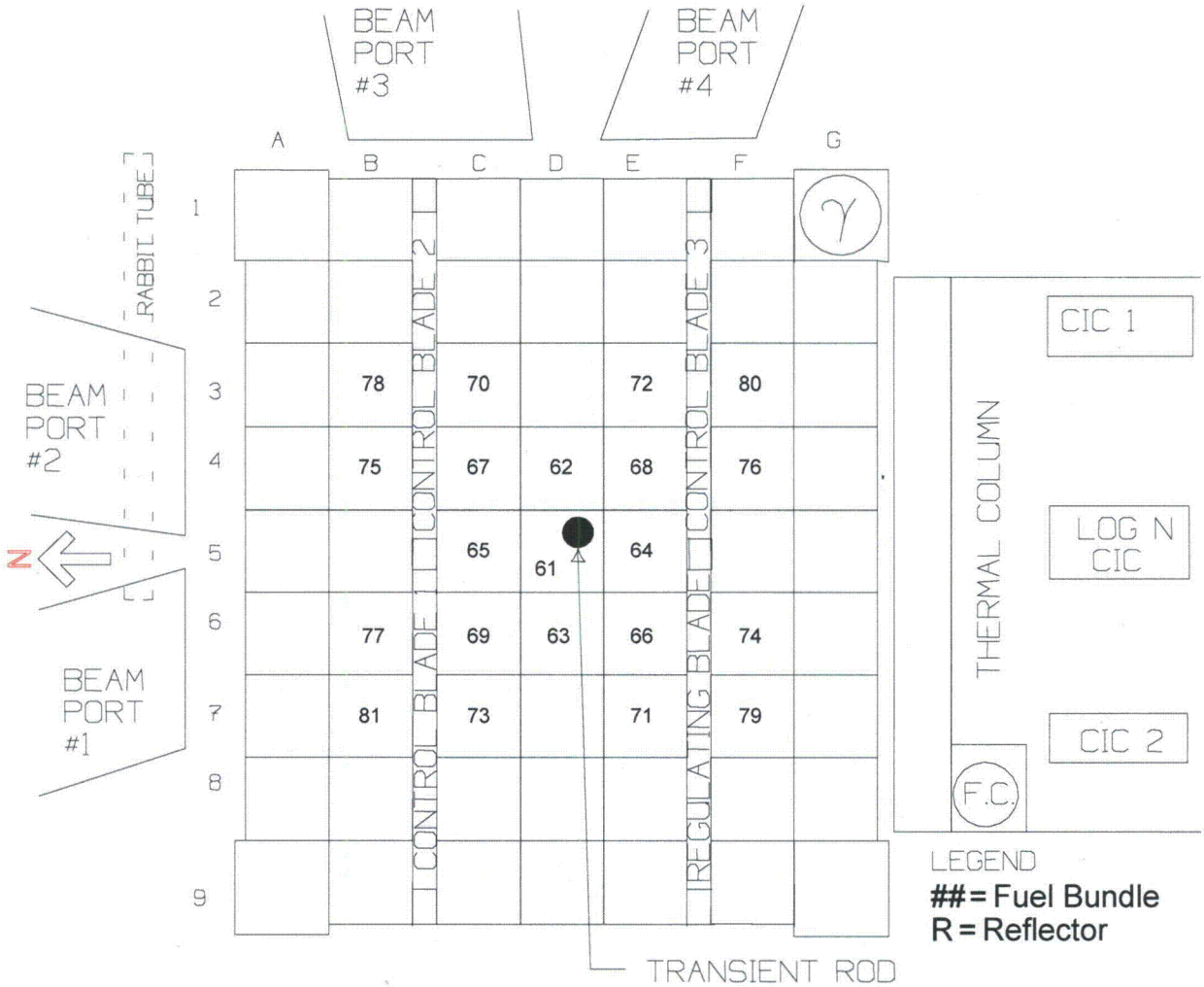

Figure 5, J21-R0 Core Map

Table 5, Measured 1/M Count Data Continued (no reflectors installed)

Bundle Added	Total	Bank full in			Bank half out		
		FC	AFC	Min	FC	AFC	Min
F7	19	3543	4347	10	3302	7295	5
F3	20	4328	5125	10	4504	9828	5

Table 6, Calculated 1/M Values Continued (no reflectors installed)

Total Bundles	Bank full in		Bank half out	
	1/M FC	1/M AFC	1/M FC	1/M AFC
19	0.285	0.051	0.141	0.011
20	0.233	0.043	0.103	0.009

Measurements of absolute and technical specification shutdown margin were made at each critical configuration, as indicated in Table 7. Reactivity was determined using the rod drop method.

Table 7, Rod Drop Measurements of Shutdown Margin (no reflectors installed)

Number Bundles	Measured Bank Height [inches]	Rod Drop True SDM [%Δk/k]	Rod Drop T.S. SDM [%Δk/k]
18	17.04	> 8.81*	5.26
19	14.83	8.41	4.40
20	13.66	8.43	3.36
21	12.83	8.08	3.19

* Insufficient excess reactivity to make reactor critical without using a non scrammable control element

After loading to the J21-R0 core, control element differential worths were measured using the rising period rod bump method. The measured data and worth curves are shown in Table 8 and Figure 6 through Figure 10, with the integral worths, shutdown margin and excess reactivity summarized in Table 9.

Table 8, J21-R0 Differential Rod Worth Data

Starting Height [inches]	Ending Height [inches]	Average Height [inches]	Doubling Time [sec]	Reactivity Worth [%Δk/k]	Differential Worth [%Δk/k/in]
Blade 1					
5.16	5.80	5.480	58.82	0.0785	0.1226
7.00	7.68	7.340	32.80	0.1190	0.1750
9.00	9.86	9.430	18.08	0.1722	0.2003
10.50	11.34	10.920	22.30	0.1522	0.1811
12.50	13.34	12.920	35.26	0.1134	0.1350
14.50	15.35	14.925	76.60	0.0639	0.0752
Blade 2					
5.06	5.92	5.490	35.68	0.1125	0.1308
7.00	7.80	7.400	25.83	0.1390	0.1737
9.00	9.79	9.395	21.58	0.1552	0.1965
10.50	11.33	10.915	23.39	0.1478	0.1781
12.50	13.31	12.905	42.07	0.1003	0.1238
14.50	15.42	14.960	79.76	0.0619	0.0673
Blade 3					
4.01	5.12	4.565	38.10	0.1075	0.0968
6.00	6.85	6.425	30.14	0.1259	0.1481
9.00	9.80	9.400	23.23	0.1485	0.1856
11.50	12.33	11.915	32.40	0.1200	0.1446
13.00	14.22	13.610	33.14	0.1182	0.0969
14.25	16.16	15.205	39.90	0.1041	0.0545
Regulating Blade					
1.50	3.43	2.465	343.72	0.0172	0.0089
5.00	6.86	5.930	105.85	0.0491	0.0264
8.00	8.87	8.435	204.11	0.0277	0.0319
11.00	12.08	11.54	210.13	0.0270	0.0250
13.50	15.16	14.33	288.24	0.0202	0.0122
Transient Rod					
Unlatched	10.64	N/A	9.88	0.2372	N/A
10.75	11.60	11.175	8.86	0.2499	0.2940
11.00	11.87	11.435	9.26	0.2448	0.2813
12.50	13.41	12.955	14.37	0.1957	0.2151
13.50	14.41	13.955	22.62	0.1509	0.1658
15.50	16.57	16.035	55.60	0.0819	0.0765

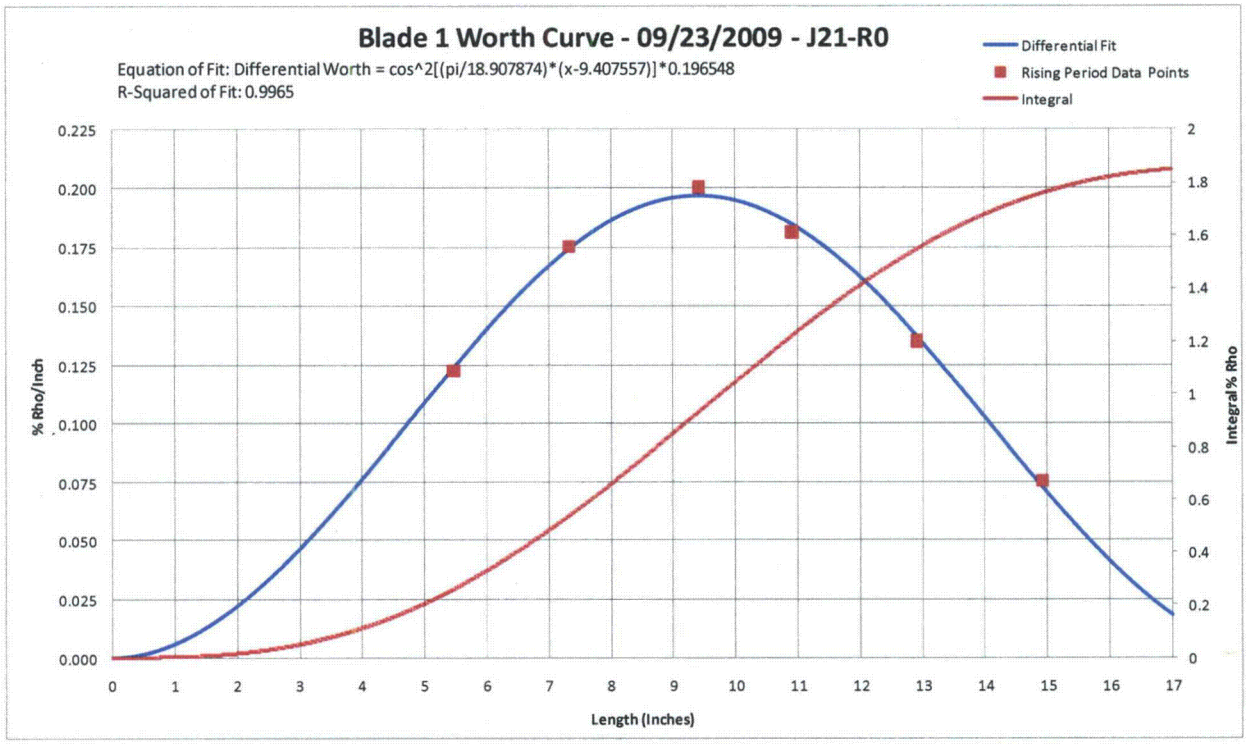

Figure 6, J21-R0 Blade 1 Worth Curves

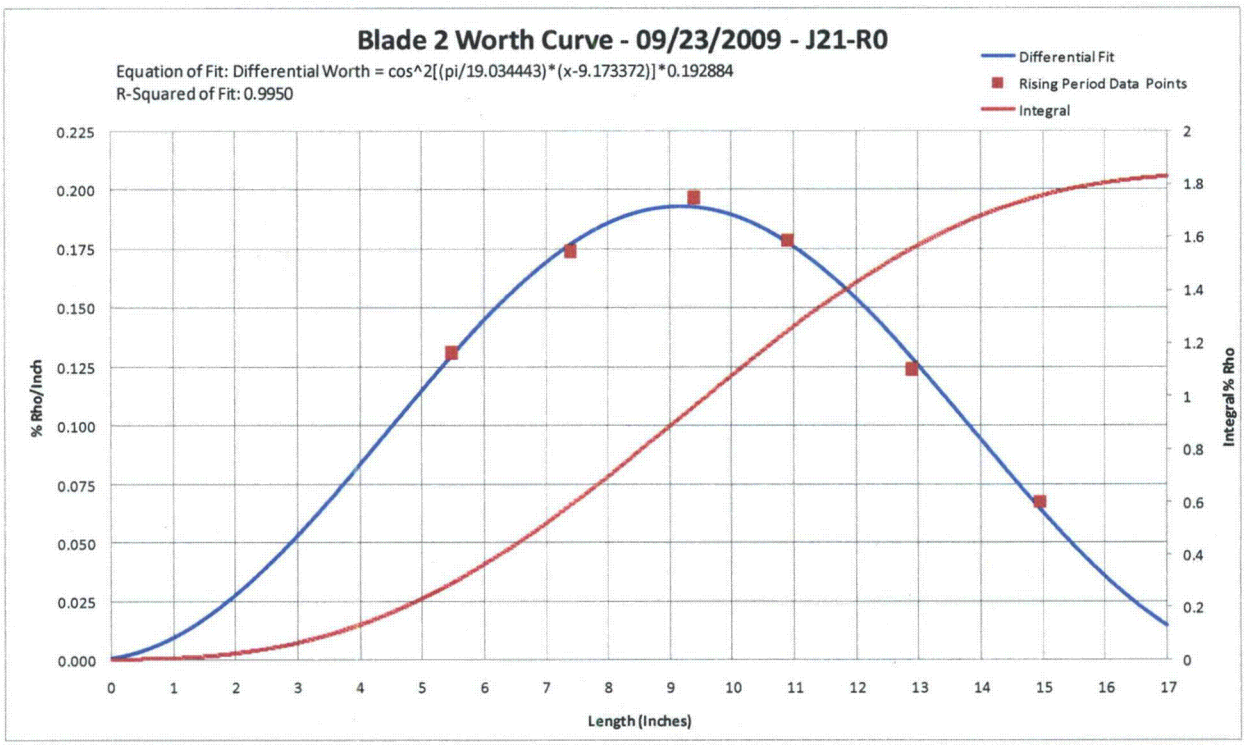

Figure 7, J21-R0 Blade 2 Worth Curves

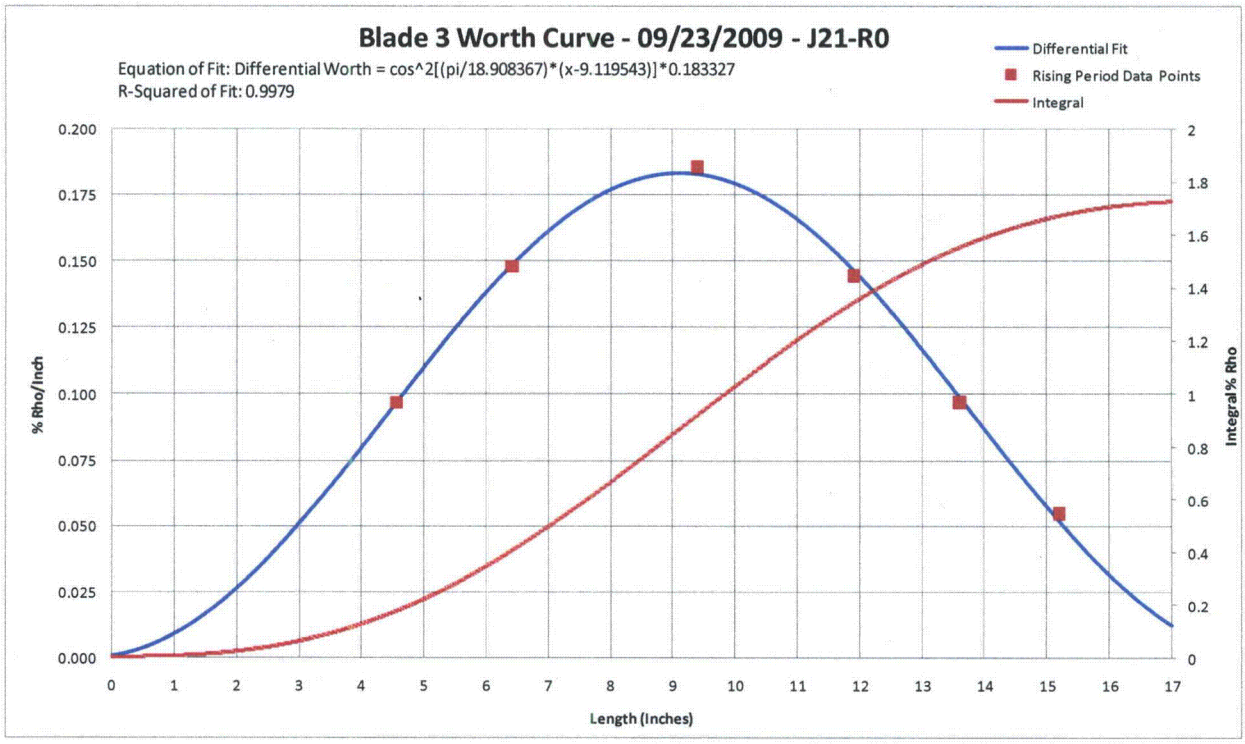

Figure 8, J21-R0 Blade 3 Worth Curves

Figure 9, J21-R0 Regulating Blade Worth Curves

Figure 10, J21-R0 Transient Rod Worth Curves

Table 9, J21-R0 Control Element Calibration

J21-R0 Core Parameter	Measured [%Δk/k]
Blade 1 worth (rod bump)	1.847
Blade 2 worth (rod bump)	1.827
Blade 3 worth (rod bump)	1.727
Regulating blade worth (rod bump)	0.308
Transient rod worth (rod bump)	1.390
Core excess reactivity	1.473
True shutdown margin (rod bump)	5.598
True shutdown margin (rod drop)	8.08
Technical specification shutdown margin (rod bump)	3.585
Technical specification shutdown margin (rod drop)	3.19

Based on the rod calibration data, the worth of each reflector position was measured by loading one reflector and noting the change in critical bank height. Reactivity worths are shown in Figure 11 for the unreflected configuration. During these measurements, some difficulty was encountered fully seating some reflector positions, and those remaining reflectors which had not been irradiated were shipped out to have the bases machined to a narrower width. In the meantime, reflector position B5 was chosen as a reference location to test the worth of several

reflectors due to its high reactivity worth. The testing demonstrated that not only were multiple new reflectors identical in worth, but they were also identical in worth to the old reflectors. Therefore, reflector worth measurements resumed using reflector R11 for the final five measurements.

	A	B		C	D	E		F	G
3	0.012		Blade 2		0.223		Blade 3		0.019
4	0.025								0.064
5	0.038	0.369						0.419	0.064
6	0.032		Blade 3				Regulating Blade		0.057
7	0.006				0.237				0.025

Figure 11, Un-reflected Reflector Reactivity Worths [%Δk/k]

E. LOADING TO J21-R14 OPERATIONAL CORE

After summing each individual reflector worth from Figure 11 to verify shutdown margin would meet requirements, reflectors were added in 4 steps, with a rod drop measurement of technical specification shutdown margin after each step. Reflector positions at each step are shown in through Figure 15. The measurements of technical specification shutdown margin at each step are summarized in Table 10. Old reflectors were used as place-holders for those new reflectors still being machined.

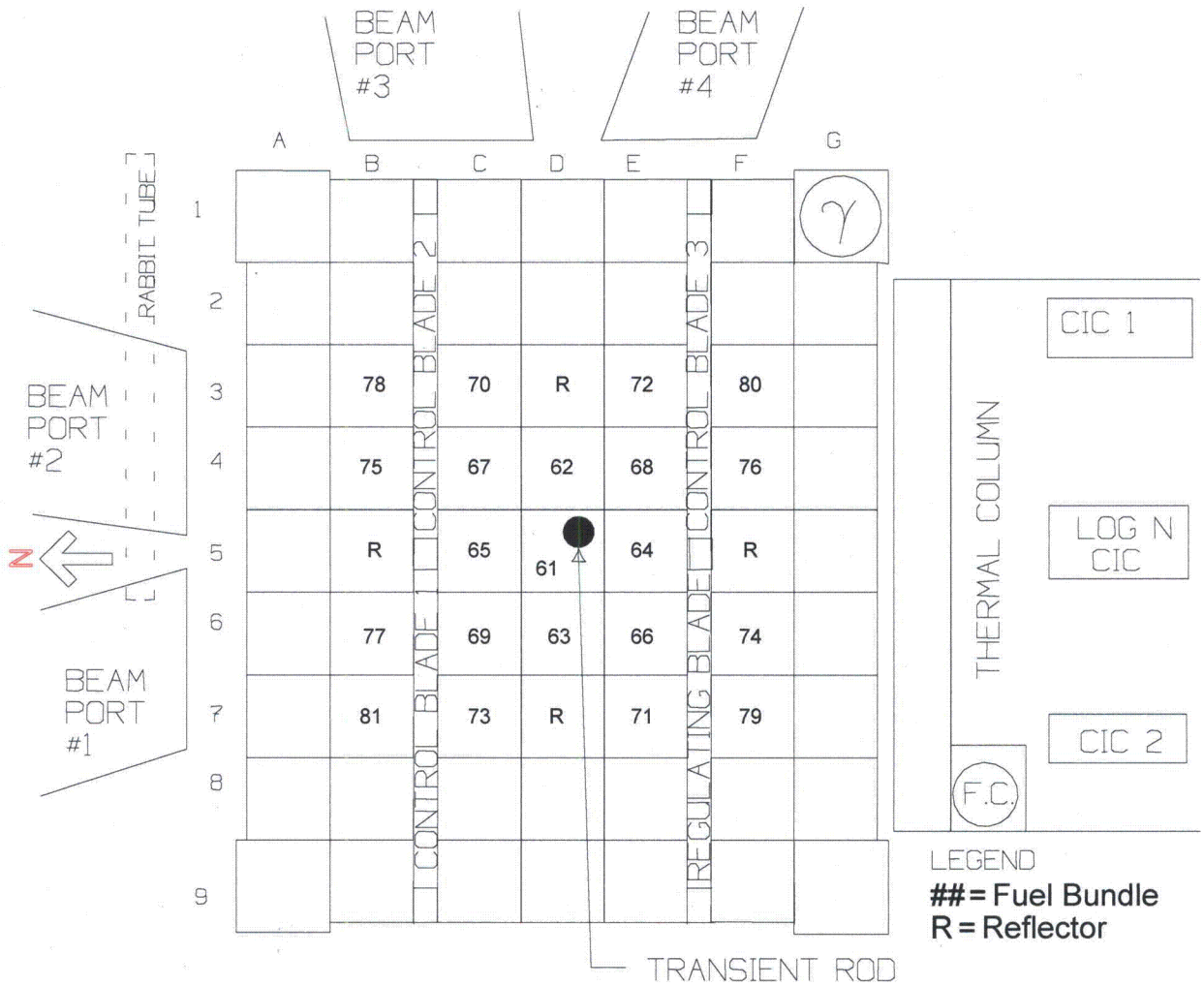

Figure 12, J21-R4 Intermediate Core Map, T.S. SDM = 2.20 %Δk/k (rod drop)

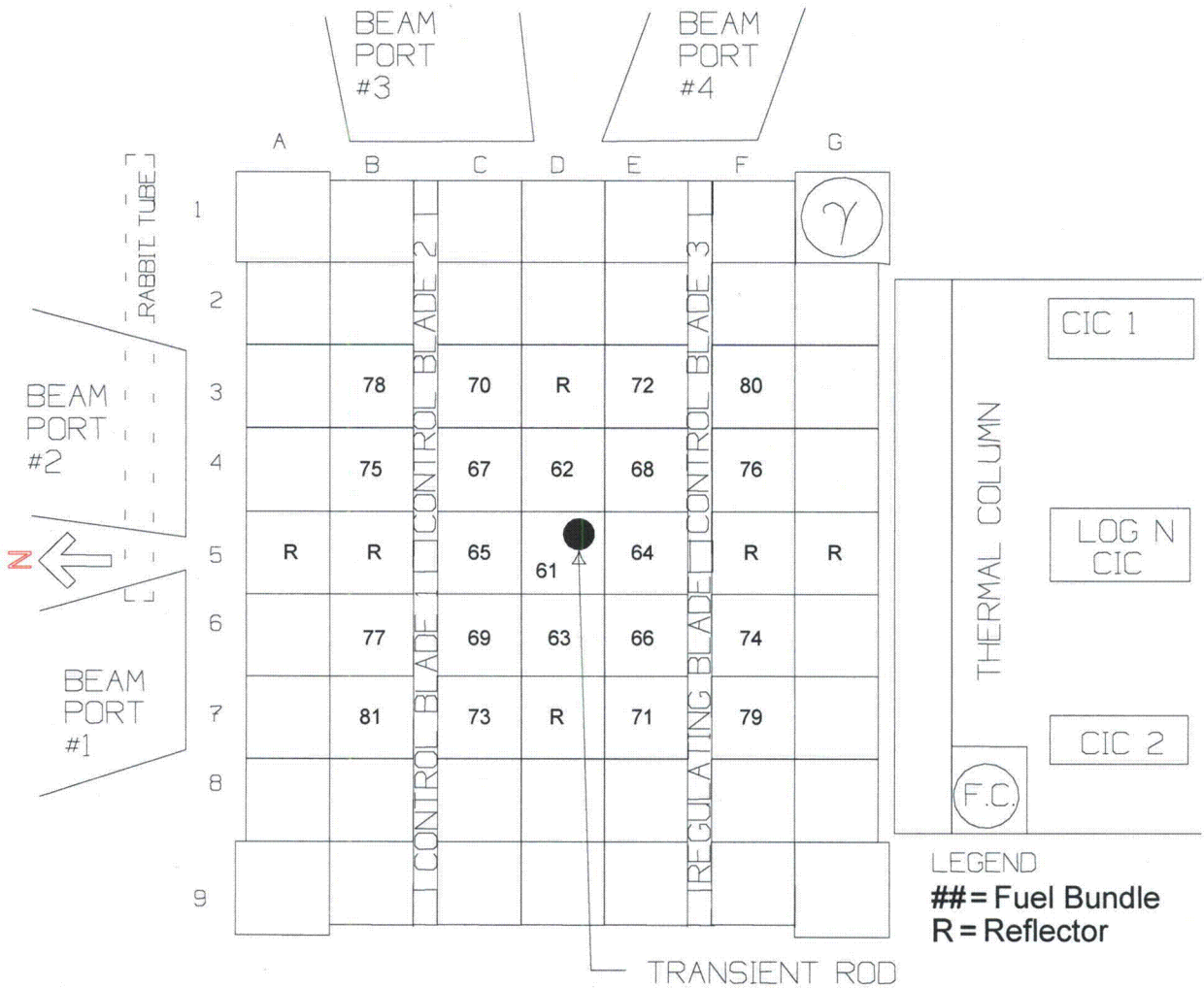

Figure 13, J21-R6 Intermediate Core Map, T.S. SDM = 1.99 %Δk/k (rod drop)

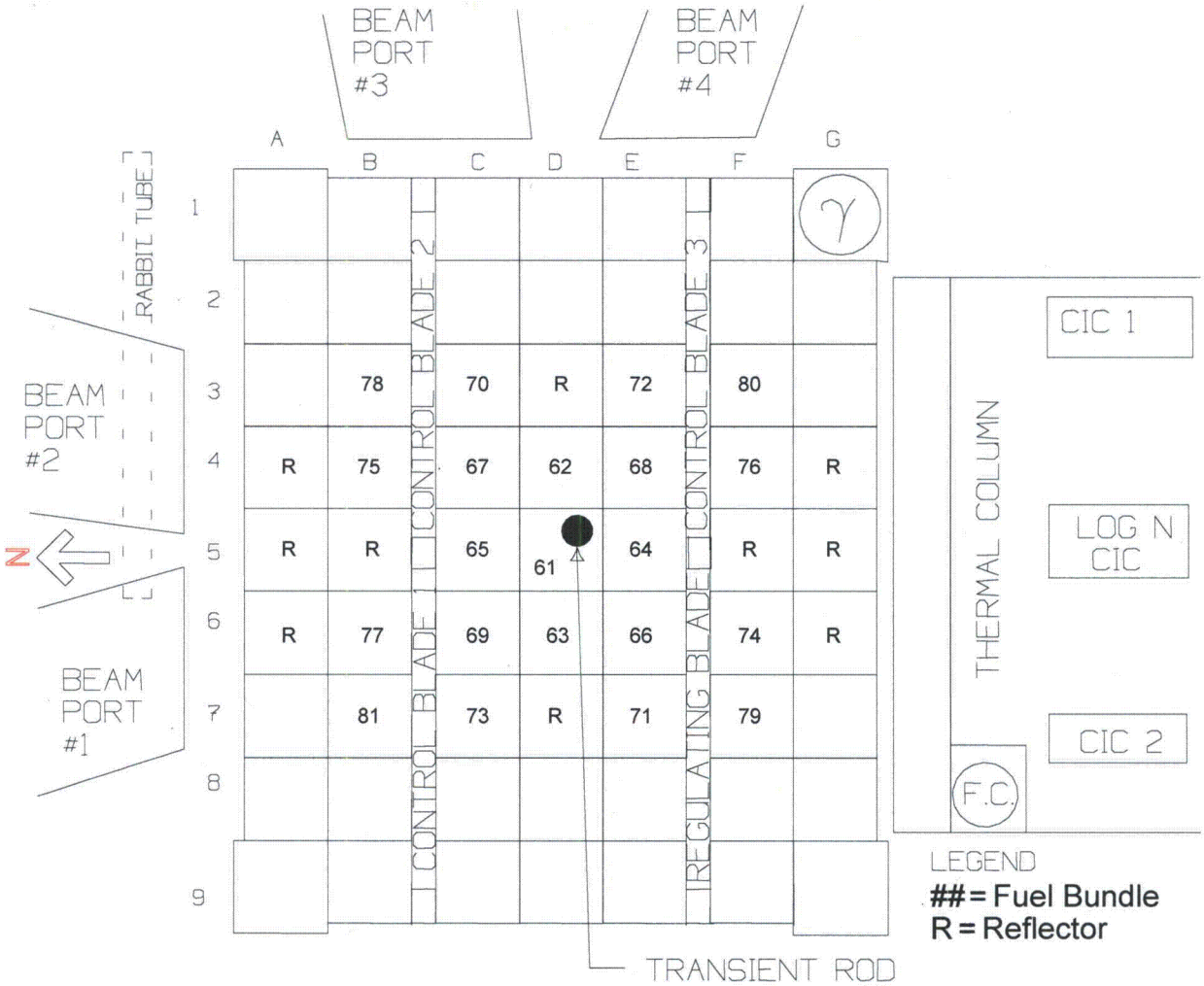

Figure 14, J21-R10 Intermediate Core Map, T.S. SDM = 1.62 %Δk/k (rod drop)

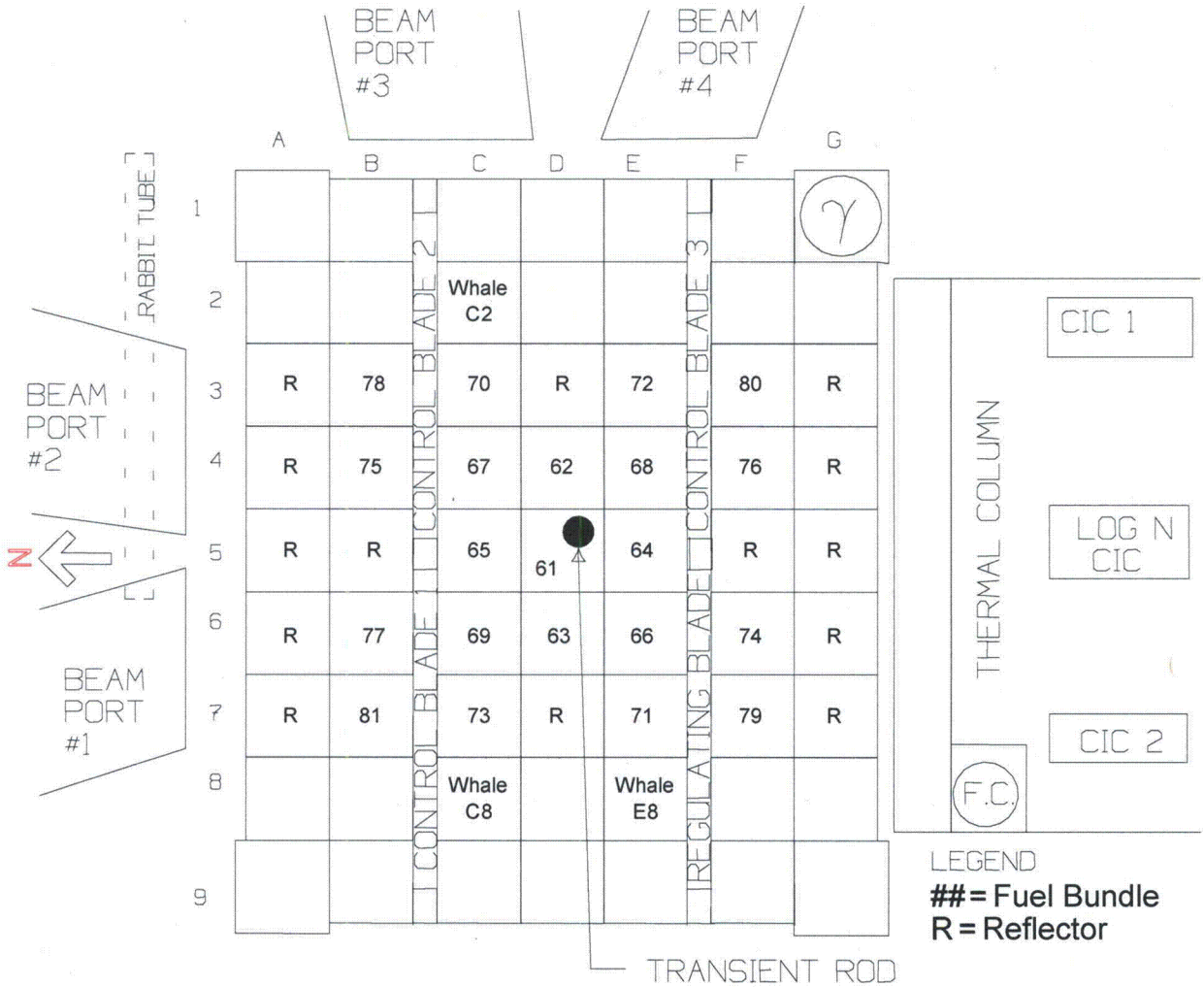

Figure 15, J21-R14 Operational Core Map, T.S. SDM = 1.39 %Δk/k (rod drop)

Table 10, SDM Measurements during Reflector Loading

Core Loading	Rod Drop Technical Specification Shutdown Margin [%Δk/k]
J21-R0	3.19
J21-R4	2.20
J21-R6	1.99
J21-R10	1.62
J21-R14	1.39

The first J21-R14 core was loaded on September 30, 2009, with a technical specification shutdown margin of 1.390 %Δk/k measured with the rod drop method. The critical bank height was 10.19 inches at 100W. Control element differential worths were again determined using the rising period rod bump method on the J21-R14 core. The measured data and differential worth curves are shown in Table 11 and Figure 16 through Figure 20, with the integral worths, shutdown margin and excess reactivity summarized in Table 12.

Table 11, J21-R14 Differential Rod Worth Data

Starting Height [inches]	Ending Height [inches]	Average Height [inches]	Doubling Time [sec]	Reactivity Worth [%Δk/k]	Differential Worth [%Δk/k/in]
Blade 1					
1.50	2.33	1.915	132.92	0.0405	0.0488
2.50	3.44	2.970	62.06	0.0753	0.0801
3.50	4.32	3.910	54.40	0.0832	0.1015
4.50	5.33	4.915	34.60	0.1148	0.1383
5.50	6.31	5.905	24.24	0.1446	0.1785
6.50	7.28	6.890	21.06	0.1575	0.2020
7.50	8.43	7.965	13.48	0.2026	0.2178
8.50	9.33	8.915	15.95	0.1849	0.2228
9.50	10.34	9.920	18.69	0.1690	0.2012
10.50	11.43	10.965	15.42	0.1884	0.2025
11.50	12.31	11.905	24.08	0.1452	0.1792
12.50	13.32	12.910	32.24	0.1204	0.1468
13.50	14.38	13.940	40.54	0.1030	0.1170
14.50	15.45	14.975	54.60	0.0830	0.0874
Blade 2					
1.50	2.46	1.980	223.90	0.0255	0.0266
2.50	3.51	3.005	62.76	0.0747	0.0740
3.50	4.27	3.885	63.06	0.0744	0.0967
4.50	5.33	4.915	34.09	0.1160	0.1397
5.50	6.32	5.910	23.60	0.1470	0.1793
6.50	7.07	6.785	38.60	0.1065	0.1869
7.50	8.48	7.990	14.15	0.1974	0.2014
8.50	9.48	8.990	14.41	0.1954	0.1994
9.50	10.50	10.000	14.61	0.1940	0.1940
10.50	11.43	10.965	20.36	0.1607	0.1728
11.50	12.60	12.050	20.95	0.1580	0.1437
12.50	13.43	12.965	34.14	0.1159	0.1246
13.50	14.47	13.985	45.70	0.0945	0.0975
14.50	15.61	15.055	57.90	0.0794	0.0715

Starting Height [inches]	Ending Height [inches]	Average Height [inches]	Doubling Time [sec]	Reactivity Worth [%Δk/k]	Differential Worth [%Δk/k/in]
Blade 3					
1.50	2.49	1.995	84.44	0.0591	0.0597
2.50	3.51	3.005	50.98	0.0873	0.0865
3.50	4.41	3.955	37.89	0.1079	0.1186
4.50	5.57	5.035	19.54	0.1646	0.1539
5.50	6.27	5.885	24.28	0.1444	0.1876
6.50	7.32	6.910	17.86	0.1734	0.2115
7.50	8.17	7.835	21.62	0.1551	0.2314
8.50	9.17	8.835	22.35	0.1520	0.2269
9.50	10.19	9.845	21.02	0.1577	0.2285
10.50	11.18	10.840	25.14	0.1413	0.2079
11.50	12.23	11.865	26.66	0.1362	0.1866
12.50	13.08	12.790	48.76	0.0902	0.1555
13.50	14.29	13.895	43.82	0.0974	0.1233
14.50	15.45	14.975	53.01	0.0848	0.0893
Regulating Blade					
1.50	3.57	2.535	213.29	0.0267	0.0129
2.50	4.49	3.495	144.21	0.0377	0.0190
3.50	5.38	4.440	111.39	0.0471	0.0250
4.50	6.43	5.465	87.54	0.0574	0.0298
5.50	6.54	6.020	162.64	0.0340	0.0327
6.50	7.43	6.965	158.53	0.0347	0.0374
7.50	8.45	7.975	150.17	0.0364	0.0383
8.50	9.58	9.040	132.00	0.0407	0.0377
9.50	10.58	10.040	156.13	0.0352	0.0326
10.50	12.07	11.285	113.08	0.0465	0.0296
11.50	13.23	12.365	130.48	0.0411	0.0238
12.50	14.42	13.460	162.79	0.0339	0.0177
13.50	15.46	14.480	218.27	0.0261	0.0133
14.50	16.52	15.510	327.40	0.0180	0.0089
Transient Rod					
Unlatched	10.65	N/A	9.76	0.2387	N/A
10.75	11.50	11.125	13.01	0.2064	0.2752
11.50	12.19	11.845	17.74	0.1741	0.2524
12.50	13.15	12.825	26.85	0.1356	0.2086
13.50	14.22	13.860	32.81	0.1190	0.1653
14.50	15.42	14.960	37.55	0.1086	0.1180
15.50	17.34	16.420	31.47	0.1223	0.0665
17.50	19.14	18.320	160.79	0.0343	0.0209

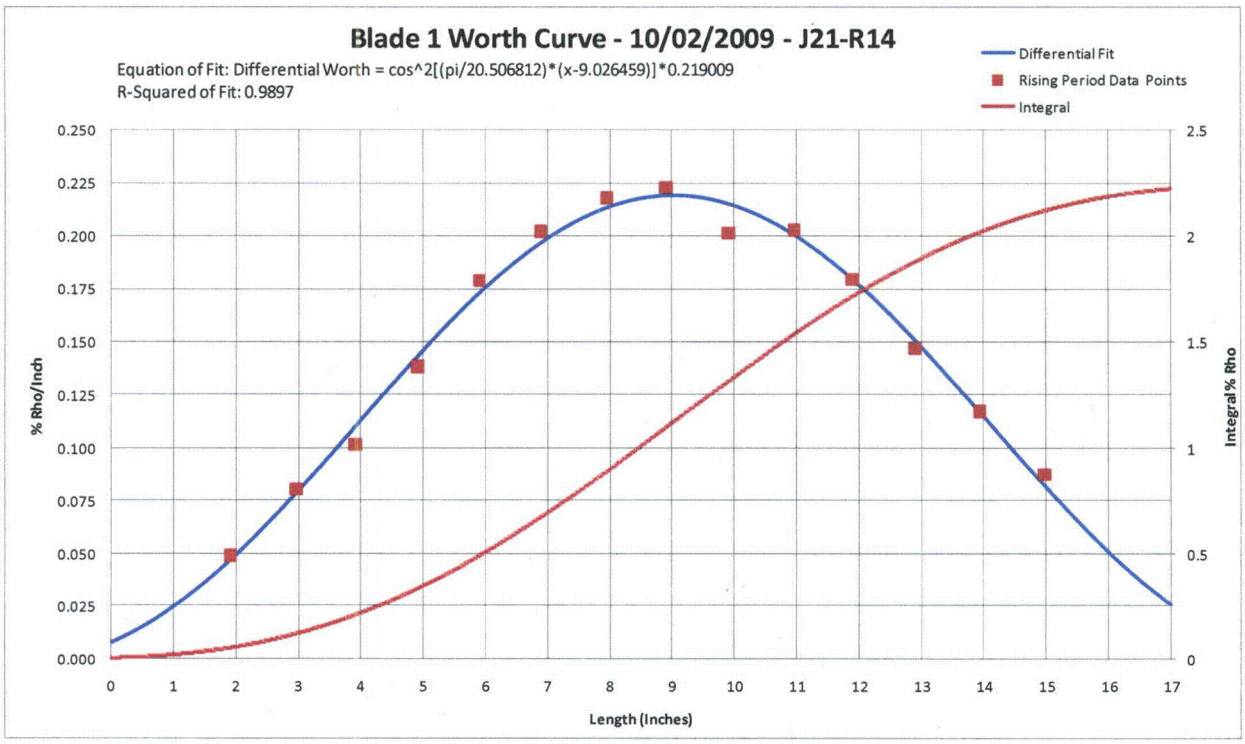

Figure 16, J21-R14 Blade 1 Worth Curves

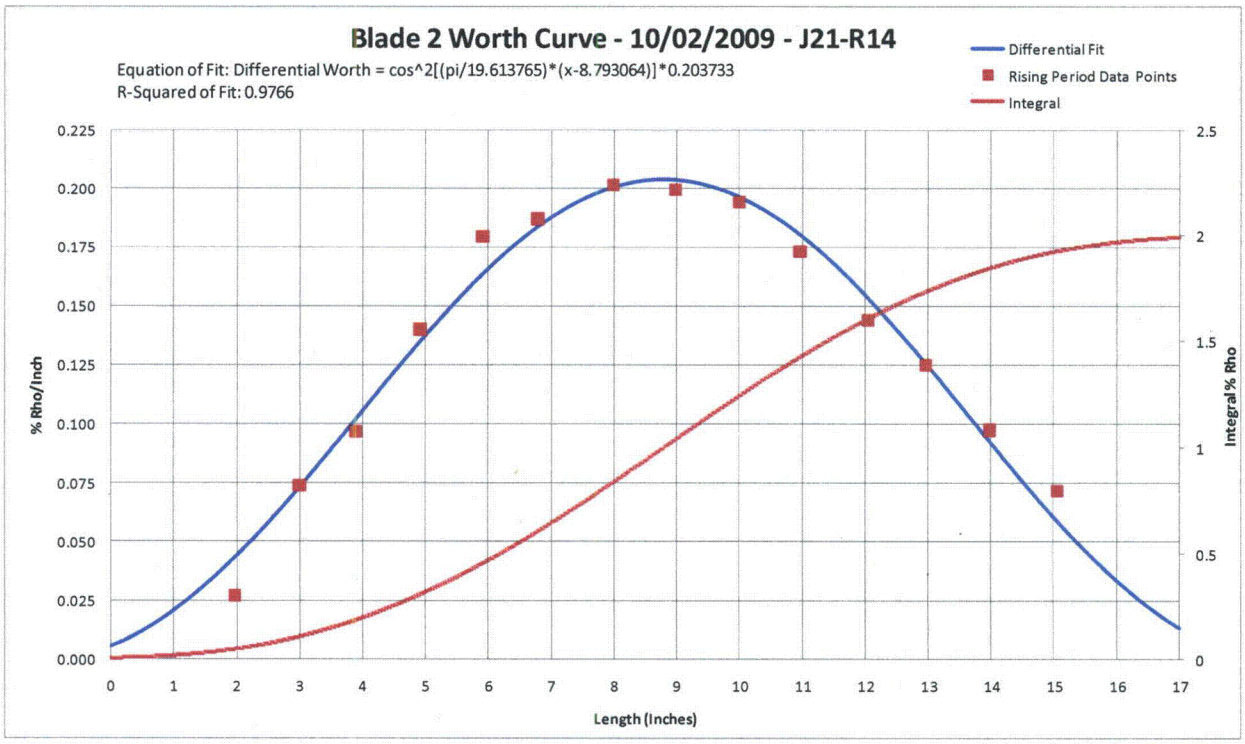

Figure 17, J21-R14 Blade 2 Worth Curves

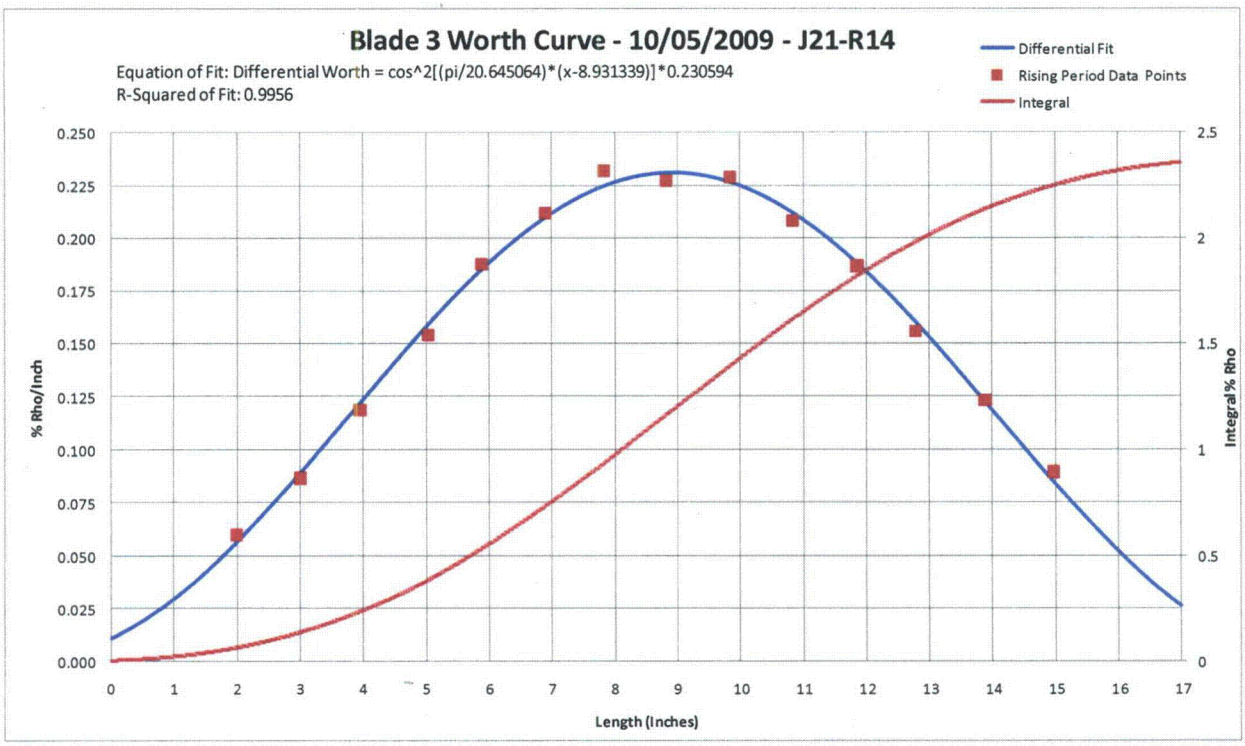

Figure 18, J21-R14 Blade 3 Worth Curves

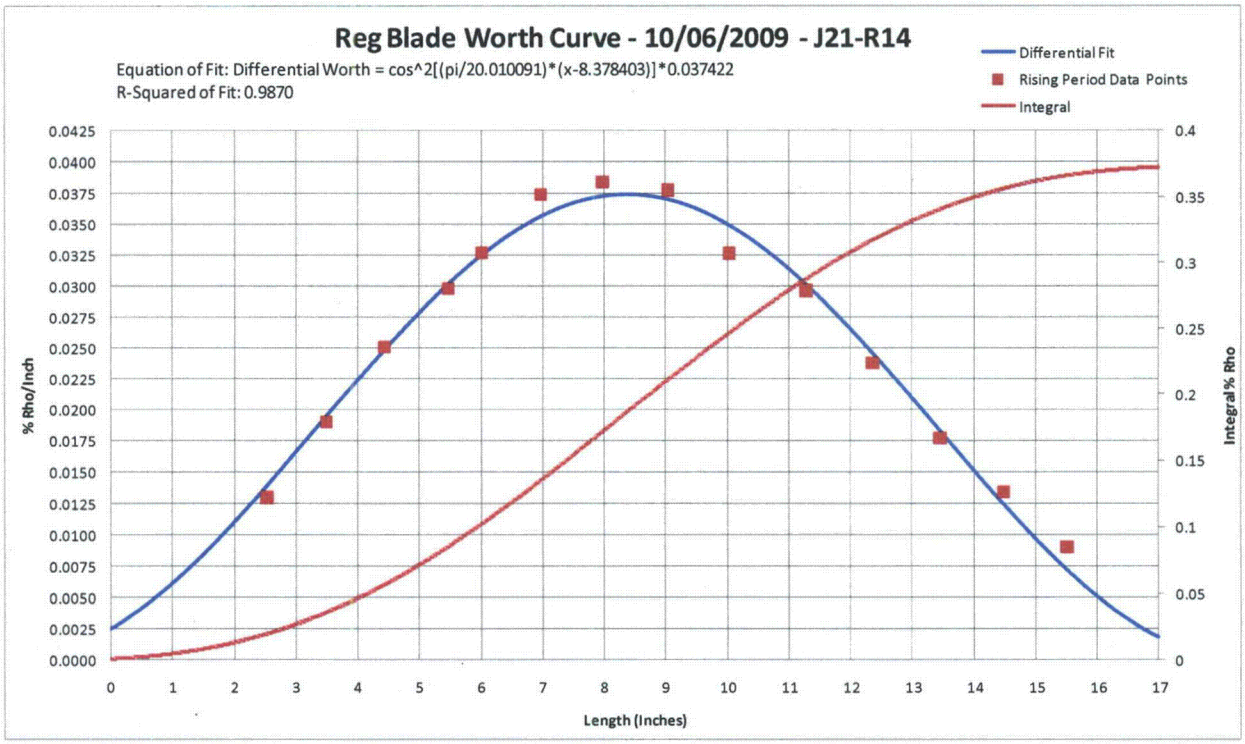

Figure 19, J21-R14 Regulating Blade Worth Curves

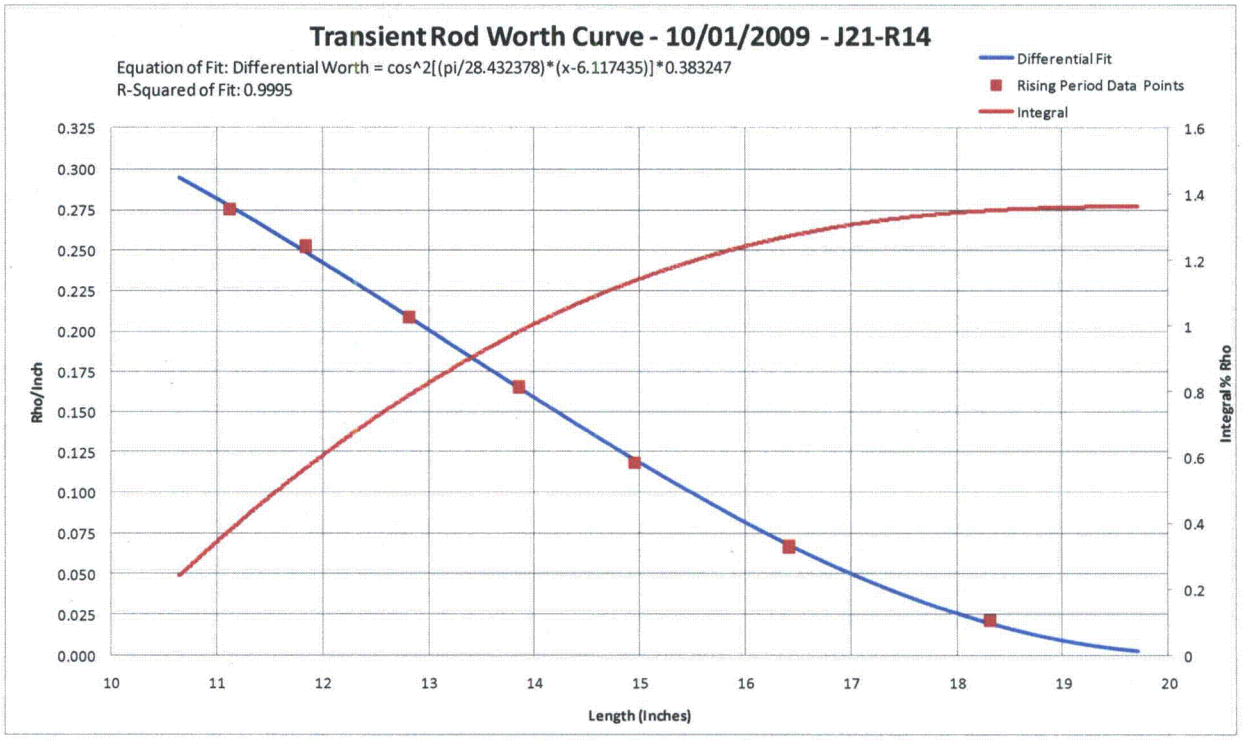

Figure 20, J21-R14 Transient Rod Worth Curves

Table 12, J21-R14 Control Element Calibration

J21-R14 Core Parameter	Measured [%Δk/k]
Blade 1 Worth (rod bump)	2.221
Blade 2 Worth (rod bump)	1.989
Blade 3 Worth (rod bump)	2.355
Regulating Blade Worth (rod bump)	0.372
Transient Rod Worth (rod bump)	1.363
Core Excess Reactivity (rod bump)	3.695
True Shutdown Margin (rod bump)	4.605
Technical Specification Shutdown Margin (rod bump)	1.779
Technical Specification Shutdown Margin (rod drop)	1.390

The hydraulic (whale) tube irradiation facilities were installed in positions C2, C8, and E8 and the critical bank height measured as 10.27 inches, a 0.08 inch increase corresponding to a reactivity worth of -0.052 %Δk/k. After receiving the re-machined reflectors, they were swapped with the old reflectors which had been loaded as place-holders. The critical bank height was measured as 10.26 inches, a 0.01 inch decrease corresponding to a reactivity worth of +0.006 %Δk/k. It was unclear whether some of the new reflectors were fully seated, so the underwater camera was used to view the installed reflectors from the side. The reflector in

position A6 was sticking up about 1/8 of an inch and was pushed down until it was fully seated. It was removed and reseated several times to verify that it did not get stuck. The critical bank height was then measured as 10.24 inches on October 9, 2009, a 0.02 inch decrease corresponding to a reactivity worth of +0.013 %Δk/k. Therefore the net change from the initial J21-R14 core at a bank height of 10.19 inches (before adding whale tubes) and the final J21-R14 core at a bank height of 10.24 inches was a 0.05 inch increase corresponding to a reactivity worth of only -0.033 %Δk/k as a result of the displacement of water with aluminum structure. Because of the small reactivity change observed, the control element calibrations for the J21-R14 core were not repeated after installation of the whale tubes.

Table 13, Predicted vs. Measured Cold Bank Height

	LEU Predicted	LEU Measured
Cold critical bank height [inches]	10.13	10.24

F. OPERATIONAL CORE REACTIVITY MEASUREMENTS

F.1 REFLECTOR REACTIVITIES (REFLECTED)

Reflectors were removed one at a time from the reflected core (making a J21 core with only 13 reflectors) to measure the reflected reactivity worths. Measured reactivities are shown in Figure 21, with the unreflected worths duplicated from Figure 11.

	A	B		C	D	E		F	G
3	R=0.025 U=0.012		Blade 2		R=0.196 U=0.223		Blade 3		R=0.072 U=0.019
4	R=0.039 U=0.025								R=0.117 U=0.064
5	R=0.052 U=0.038	R=0.347 U=0.369						R=0.494 U=0.419	R=0.150 U=0.064
6	R=0.046 U=0.032		Blade 3				Regulating Blade		R=0.137 U=0.057
7	R=0.033 U=0.006				R=0.253 U=0.237				R=0.084 U=0.025

Figure 21, Reflector Reactivity Worths [%Δk/k, R=Reflected, U=Unreflected]

F.2 COOLANT VOID COEFFICIENT

Measurements were made of the coolant void coefficient of reactivity following the procedure in UWNR 002. A total of 19 locations were used to insert aluminum wands which could be filled with water or air in order to make the measurement, but only 6 wands were ever inserted at a time to map each quadrant of the core. Refer to Figure 22. Because 3 of the locations were duplicated as each core quadrant was measured, this led to a total of 22 wands used.

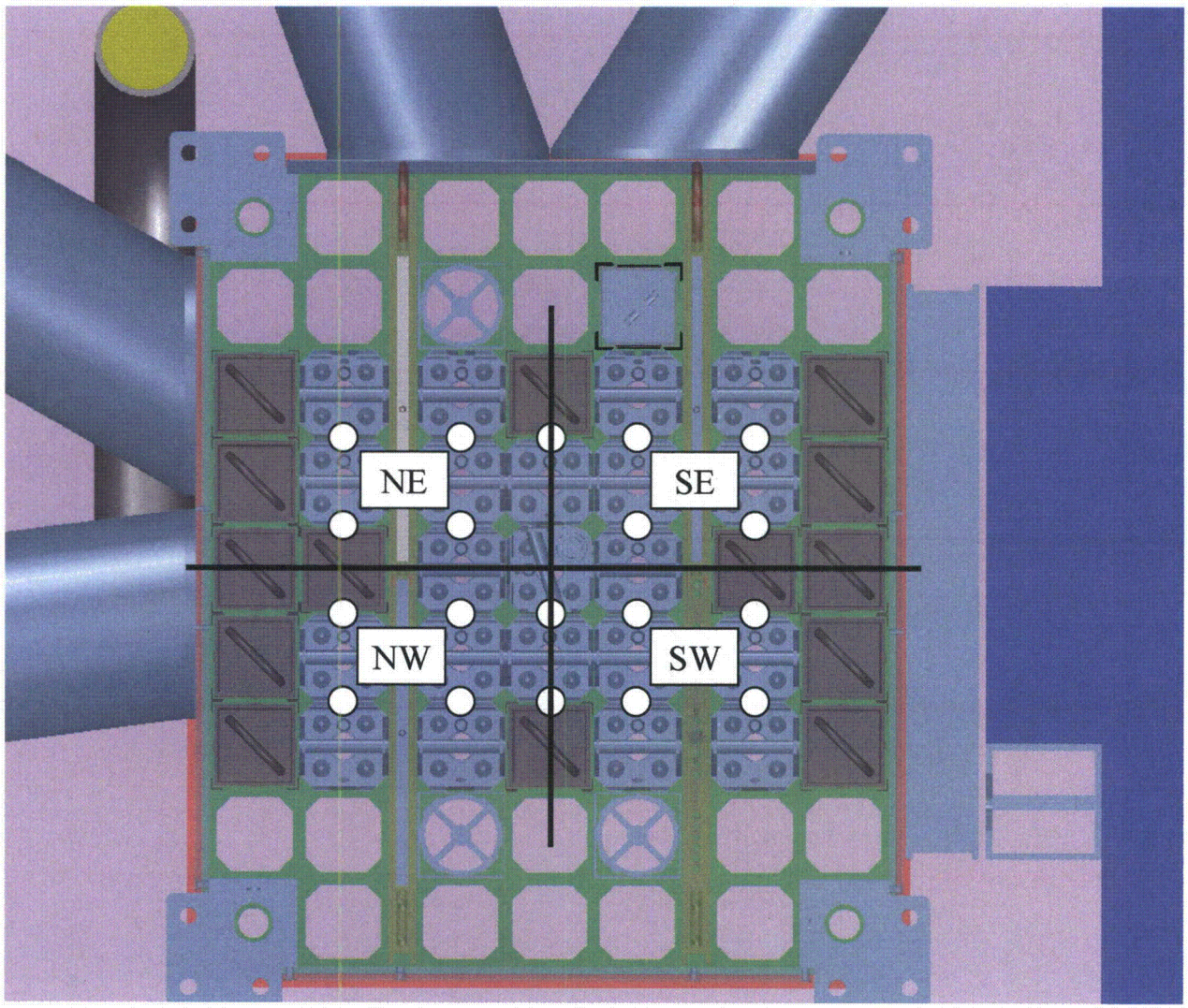

Figure 22, Air and Water Wand Locations

Static reactivity measurements were made by measuring the critical control element heights with the insertion of water filled and air filled wands. The table below shows the recorded blade heights and calculated reactivity insertion (from all blades in) based on control element calibrations.

Table 14, Water and Air Wand Reactivities

Configuration	Blade 1 Height [inches]	Blade 2 Height [inches]	Blade 3 Height [inches]	Reg. Blade Height [inches]	T-rod Height [inches]	Reactivity Inserted [%Δk/k]
SW Water Wand	10.34	10.34	10.34	10.37	10.66	4.705
SW Air Wand	10.61	10.61	10.61	10.77	10.66	4.884
NW Water Wand	10.34	10.34	10.34	10.24	10.66	4.700
NW Air Wand	10.61	10.61	10.61	10.08	10.66	4.861
NE Water Wand	10.34	10.34	10.34	9.43	10.65	4.672
NE Air Wand	10.61	10.61	10.61	7.41	10.66	4.763
SE Water Wand	10.34	10.34	10.34	9.51	10.65	4.674
SE Air Wand	10.61	10.61	10.61	7.46	10.66	4.764

The measured reactivity change in each quadrant was calculated by subtracting the reactivity insertion with air wands from the reactivity insertion with water wands. The % void fraction was calculated according to the UWNR 002 based on the number of wands used in each quadrant, the cross-sectional area of void in each wand, and the core-wide coolant cross-sectional area. The void wands are sufficiently long in the vertical direction to cover the entire region of neutron importance, so the calculated % void fraction in terms of cross-sectional areas is equivalent to the % void fraction in terms of void volume. Results for each core quadrant are shown in Table 15.

Table 15, Void Reactivity Measurements

Configuration	Reactivity Inserted [%Δk/k]	Reactivity Change [%Δk/k]	% Void	Local Void Coefficient [%Δk/k/%void]
SW Water Wand	4.705	-0.179	0.9667	-0.185
SW Air Wand	4.884			
NW Water Wand	4.700	-0.161	0.9667	-0.167
NW Air Wand	4.861			
NE Water Wand	4.672	-0.091	0.8056	-0.113
NE Air Wand	4.763			
SE Water Wand	4.674	-0.090	0.8056	-0.112
SE Air Wand	4.764			

The average coolant void coefficient of reactivity is therefore -0.14 %Δk/k/%void. Note that the measurements for the SW and NW quadrants included a wand located between D5 and D6 adjacent to the center bundle, whereas the measurements for the NE and SE quadrants could not locate a wand adjacent to the center bundle (between D4 and D5) due to interference from the transient rod guide tube. The measured reactivity change for the west quadrants was noticeably larger than the east. Although the % void fraction does account for some of the difference, the worth of the missing wand location adjacent to the center bundle is higher than the average wand location, which explains why there is still a difference in the calculated local void coefficients.

Table 16, Predicted vs. Measured Void Coefficient

	LEU Predicted	LEU Measured
Void coefficient [%Δk/k/%void]	-0.149	-0.14

F.3 EXPERIMENTAL FACILITY REACTIVITY MEASUREMENTS

Sample reactivity measurements were performed for the whale tube and pneumatic tube experimental facilities. See Table 17. The pneumatic tube was found to have very little reactivity worth with all changes well within the capability of the reactivity control system. The whale tube had higher worth as expected, but measured values were still small enough for reactivity control. Measurements were performed in whale tube E8, the highest worth location as shown in section J of this report. A number of cadmium samples were tested with varying thicknesses of cadmium wrapped along the interior of the whale bottle. The first sample had a thickness of 1mm and a total mass of 86g cadmium, and the heaviest had a thickness of 5mm and a total mass of 372g cadmium. There was no noticeable change in bank height between samples, but some variability is introduced by having the diffuser and whale pumps running. In order to observe fine differences in bank height, the lighter cadmium samples which did not sink were loaded with small amounts of lead in order to make them sink so bank heights could be measured with the diffuser and whale pumps off. Because of the low reactivity worth of the large lead sample measured, the small amounts of lead added to the cadmium whales were neglected in calculating the reactivity worth. Even with the diffuser and whale pumps off, there was no difference in bank heights between cadmium samples, demonstrating that the first 1mm layer of cadmium is essentially black to thermal neutrons.

Table 17, Predicted vs. Measured Experimental Facility Reactivities

	LEU Predicted [%Δk/k]	LEU Measured [%Δk/k]
Pneumatic Tube		
30ml water (flooding)	+0.007	+0.004
75g B_4C	N/A	-0.007
148g Cd	-0.009	-0.009
Whale Tube E8		
Air	N/A	-0.030
237g Graphite	N/A	+0.011
1464g Lead	N/A	+0.003
86-372g Cd	-0.04	-0.087

G. POWER CALIBRATIONS

The first power calibration by calorimetric heat balance was performed at 500kW as indicated by power level instrumentation, followed by a power calibration at 900kW, and finally a full power calibration at 1.00MW. Because of the results of the earlier heat balances, power level instruments were not adjusted to agree with the measurements until after the 1.00MW power calibration. Measured power levels were reasonably close and lower than the indicated power levels. See Table 18.

Table 18, Power Calibration Data

Date	Indicated Power	Actual Power
10/20/2009	500 kW	486 kW
10/26/2009	900 kW	883 kW
11/2/2009	1000 kW	979 kW

During all three power calibrations, water and air samples were taken to look for any leaking fission products using a high purity germanium detector. All air particulate samples contained Ra-224, Bi-214, and Pb-214, all naturally occurring radon decay products which are routinely detected. No other isotopes were found. All water samples contained Mg-27, Na-24, and Ar-41. Na-24 and Ar-41 are routinely detected in water samples taken at or recently after full power operations. Na-24 is produced from an n,α fast activation reaction from aluminum in the core grid box and end fittings. Ar-41 is produced from argon in the air dissolved in the pool water as it passes through the core. Mg-27 is not routinely detected, but is also produced from an n,p fast activation reaction from aluminum. It is not common to collect and count water samples during full power operations, which is why the short-lived Mg-27 is not routinely detected (half-life of 9.5 minutes). No fission products were detected in air or water samples, and no unusually high stack gas or continuous air monitor levels were observed.

After power calibrations and nuclear instrumentation adjustments were complete, the full power bank height was measured to be 12.58 inches.

Table 19, Predicted vs. Measured Hot Bank Height

	LEU Predicted Bank Height [inches]	LEU Measured Bank Height [inches]
Hot critical bank height	11.73	12.58

H. POWER DEFECT MEASUREMENTS

Power defect measurements were taken to record fuel temperature and excess reactivity vs. power level. These measurements were done in three separate days, each day beginning with a cold clean core (free of xenon). The three measurements were 0-50% in 50kW increments, 50-100% in 50kW increments, and 0-100% in 100kW increments. The raw data is shown in Table 20. The fuel temperature vs. power is shown in Figure 23 for bundle 62 and Figure 24 for bundle 72. By using the recorded bank heights along with the J21-R14 control element calibration curves, the excess reactivity vs. power was calculated and is shown in Figure 25. The maximum reading thermocouple, bundle 62 center, was also used to plot fuel temperature vs. excess reactivity in Figure 26. The data from all three days shows good agreement indicating that no significant amount of xenon had built up during each day's measurements.

Table 20, Temperature vs. Power Measurements

Power Level [kW]				Bank Height [inches]	Bundle 62 D4 SW [°C]			Bundle 72 E3 NE [°C]		
kW	pA #1	pA #2	LogN		Bottom	Center	Top	Bottom	Center	Top
0-50% in 50kW increments										
<1	0.30	0.32	0.40	10.36						
50	47	50	50	10.64	71.2	70.2	67.7	57.1	56.7	54.1
100	98	100	90	10.82	107.3	106.2	101.0	88.3	88.3	83.9
150	150	150	160	10.98	140.9	139.8	132.6	115.8	115.6	108.6
200	200	200	210	11.13	167.3	166.2	156.8	137.9	137.4	129.8
250	240	250	280	11.26	181.8	178.7	167.4	158.6	157.8	148.9
300	290	300	300	11.36	195.3	193.1	181.6	178.4	177.8	167.8
350	340	350	360	11.44	201.8	201.0	189.4	193.9	191.5	180.9
400	380	400	400	11.52	209.6	211.7	199.6	208.3	205.8	195.2
450	430	450	450	11.60	221.2	224.4	213.3	220.9	218.0	207.3
500	470	500	500	11.67	231.4	235.6	224.2	230.7	227.3	216.4
50-100% in 50kW increments										
<1	0.28	0.32	0.40	10.39	25.9	25.8	25.8	25.3	25.2	25.2
500	470	500	500	11.66	226.0	229.9	220.2	222.2	224.8	215.8
550	520	550	550	11.74	235.9	241.9	232.5	232.6	233.8	225.0
600	570	600	600	11.82	246.5	253.8	245.2	239.3	240.5	233.7
650	620	650	650	11.89	255.9	265.8	257.6	247.4	248.7	242.1
700	670	700	700	11.96	265.3	277.8	270.7	252.5	257.1	252.9
750	730	750	800	12.04	274.4	288.4	281.4	262.4	268.6	263.9
800	780	800	850	12.12	282.6	298.7	291.8	272.0	278.2	273.7
850	840	850	900	12.21	293.4	311.1	303.3	285.2	291.9	286.0
900	890	900	950	12.30	303.0	322.3	314.4	297.6	303.0	296.0
950	940	950	950	12.38	312.4	333.2	325.0	309.7	314.3	306.1
1000	1000	1000	1000	12.47	320.6	342.6	334.1	318.6	323.4	314.2
0-100% in 100kW increments										
<1	0.36	0.39	0.50	10.37	25.8	25.7	25.6	25.2	24.9	25.0
100	100	100	100	10.82	112.7	111.2	105.4	88.2	89.6	87.7
200	190	200	200	11.11	165.8	162.4	152.4	131.0	134.0	131.6
300	290	300	300	11.35	194.4	190.1	178.4	170.6	174.6	169.3
400	380	400	400	11.51	207.3	206.3	196.3	200.0	204.3	196.2
500	470	500	500	11.66	225.2	231.2	221.8	223.6	225.5	216.0
600	570	600	600	11.81	247.2	255.1	246.9	240.7	242.8	234.2
700	670	700	700	11.96	265.7	277.7	270.1	252.7	256.5	251.7
800	780	800	850	12.11	283.0	298.9	291.4	272.1	277.6	273.1
900	890	900	950	12.29	303.4	322.6	314.1	295.4	301.4	294.7
1000	1000	1000	1000	12.47	320.2	342.8	334.4	318.2	322.3	312.7

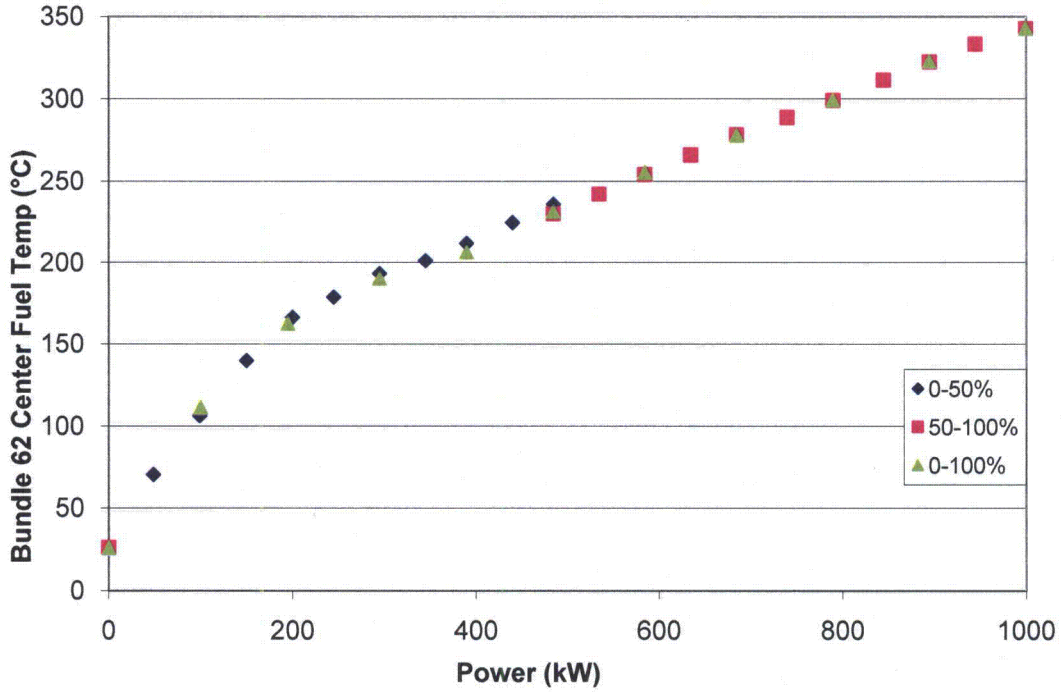

Figure 23, Bundle 62 Fuel Temperature vs. Power

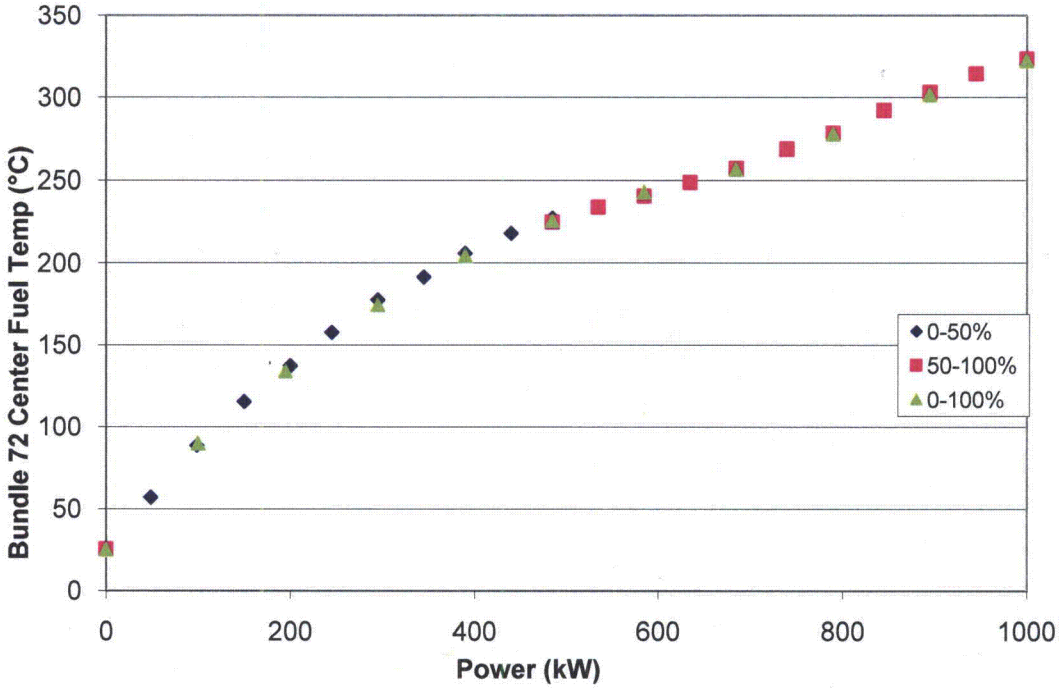

Figure 24, Bundle 72 Fuel Temperature vs. Power

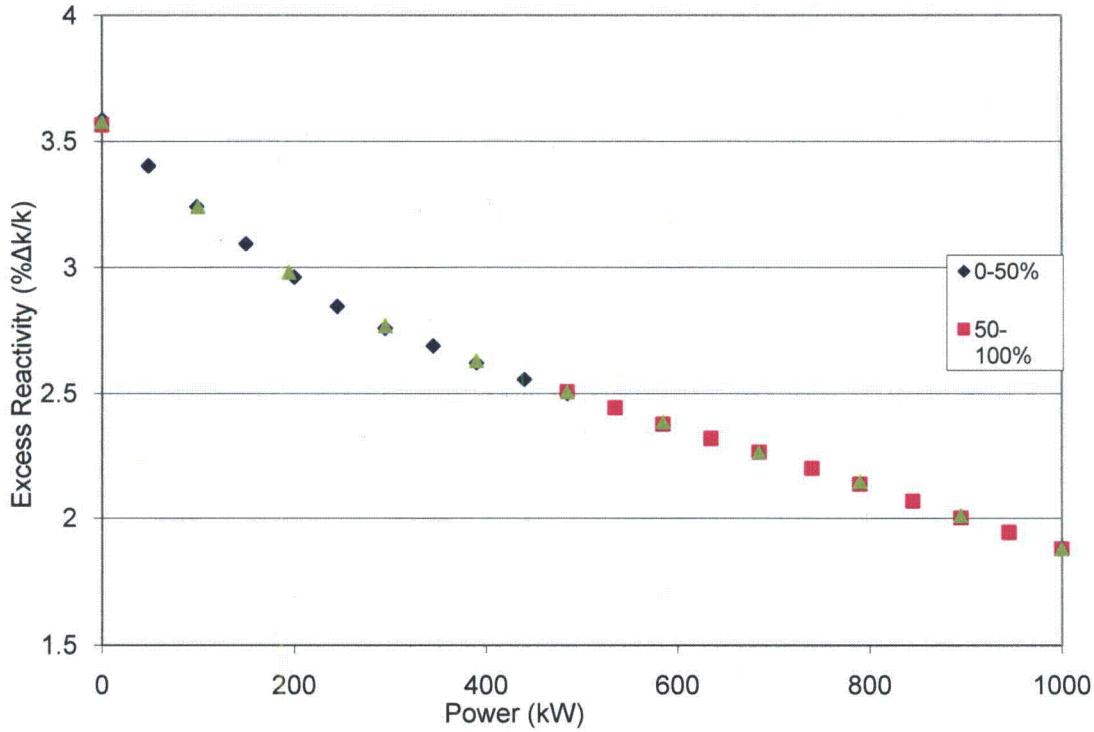

Figure 25, Excess Reactivity vs. Power

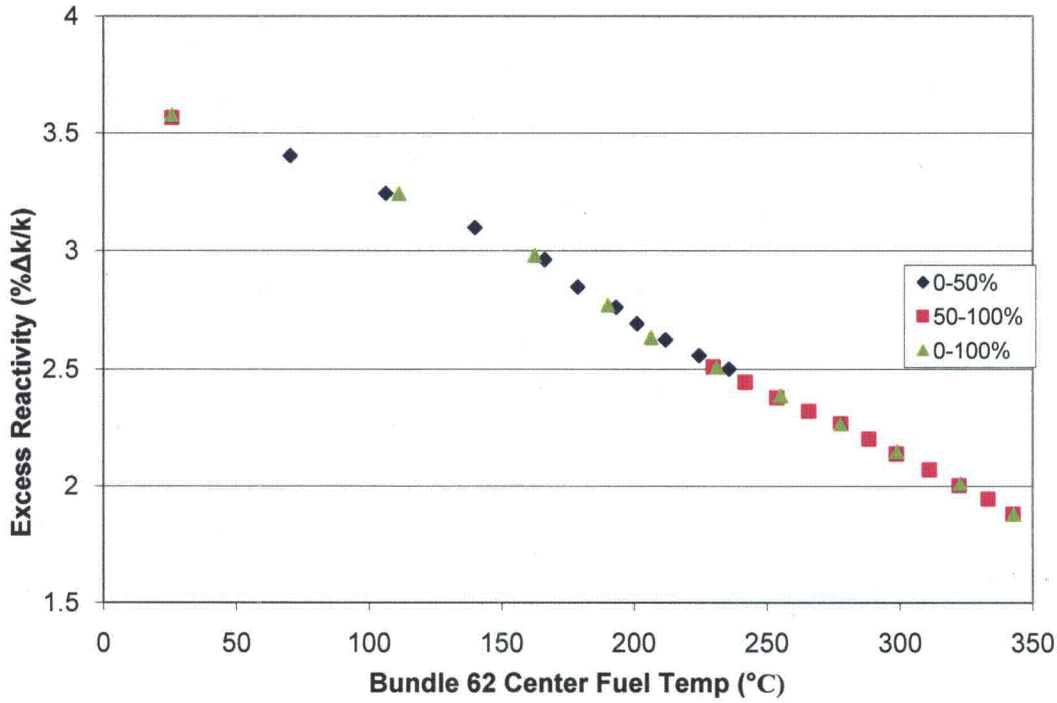

Figure 26, Excess Reactivity vs. Bundle 62 Fuel Temperature

The linear trend of excess reactivity vs. power does not begin until power is greater than 350kW. Using the data greater than 350kW, the power defect is calculated to be -1.22×10^{-3} %Δk/k/kW with an R^2 of 1.000, and the fuel temperature coefficient is calculated to be -5.55×10^{-3} %Δk/k/°C with an R^2 of 0.998 (using the highest reading thermocouple in bundle 62 center).

Table 21, Predicted vs. Measured Temperature Coefficients

	LEU Predicted	LEU Measured
Power defect [%Δk/k/kW]	N/A	-1.22×10^{-3}
Fuel temperature coefficient [%Δk/k/°C]	-4.08×10^{-3} (300-400K) -6.58×10^{-3} (400-600K)	-5.55×10^{-3}

I. FUEL TEMPERATURE MAPPING

The IFE in bundle 62 was moved into every available core location in order to map the temperature across the core. Only the D5 location was not mapped because of the transient rod bundle. The IFE in bundle 72 was also moved into 5 different locations to compare to the bundle 62 data. All measurements were performed with the thermocouple facing east for consistency. Figure 27 through Figure 29 show the temperature distributions across the core for top, center, and bottom thermocouples in bundle 62. Table 22 compares measured temperatures between bundle 72 and 62.

Table 22, Fuel Temperature Mapping Data, Bundle 72 vs. Bundle 62

Position	Bundle 72 [°C]			Bundle 62 [°C]			Difference 72-62 [°C]		
	Top	Center	Bottom	Top	Center	Bottom	Top	Center	Bottom
D4 SW	388.3	405.3	402.2	334.6	342.3	318.9	53.7	63.0	83.3
D4 SE	376.0	391.1	388.8	320.9	324.4	305.4	55.1	66.7	83.4
D4 NE	377.2	391.1	388.4	317.9	320.9	302.0	59.3	70.2	86.4
D4 NW	390.9	410.9	410.7	325.1	330.6	309.1	65.8	80.3	101.6
E3 NE	303.3	318.6	317.4	265.0	269.1	257.2	38.3	49.5	60.2

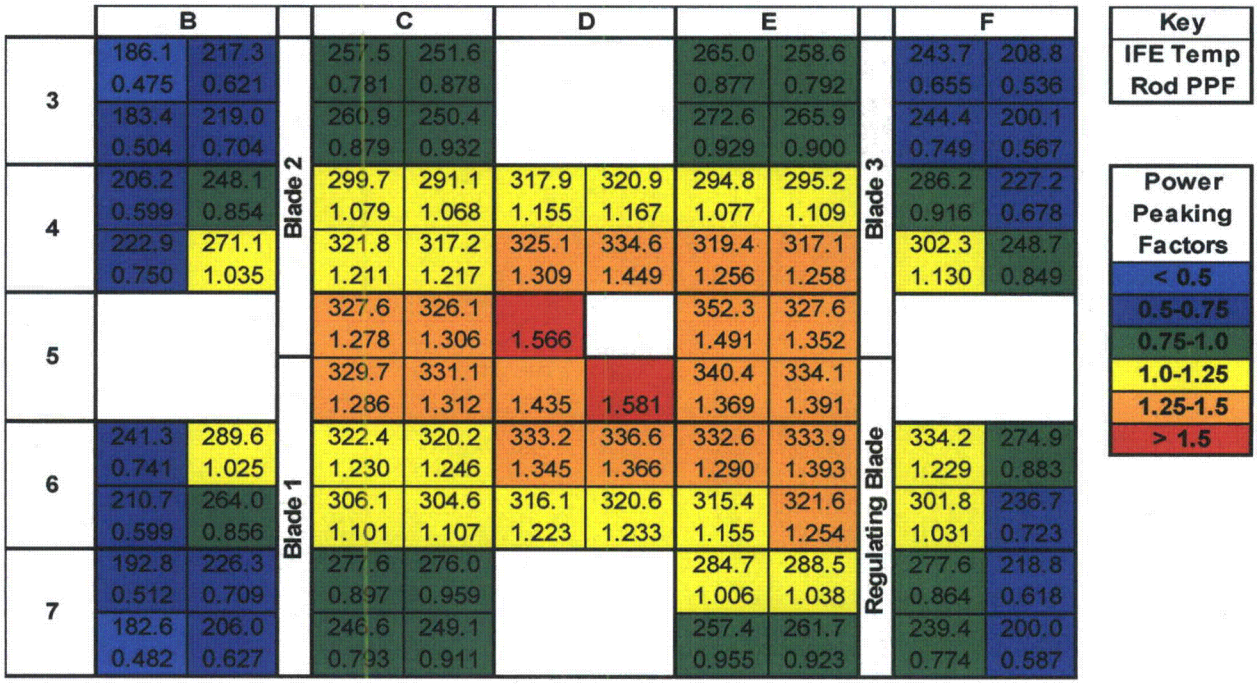

Figure 27, Bundle 62 Top Measured IFE Temperature Distribution at 1.0MW

	B			C		D		E			F	
3	192.1 0.475	224.2 0.621		265.4 0.781	257.2 0.878			269.1 0.877	263.2 0.792		250.9 0.655	210.8 0.536
	186.0 0.504	223.0 0.704		267.4 0.879	255.2 0.932			276.0 0.929	270.8 0.900		252.8 0.749	202.6 0.567
4	208.1 0.599	255.3 0.854	Blade 2	307.3 1.079	295.7 1.068	320.9 1.155	324.4 1.167	298.4 1.077	301.0 1.109	Blade 3	291.5 0.916	229.1 0.678
	226.2 0.750	277.0 1.035		328.9 1.211	322.0 1.217	330.6 1.309	342.3 1.449	324.6 1.256	322.2 1.258		306.0 1.130	248.9 0.849
5				333.2 1.278	331.1 1.306	1.566		365.1 1.491	331.8 1.352			
				335.4 1.286	335.6 1.312	1.435	1.581	347.9 1.369	338.0 1.391			
6	243.5 0.741	296.6 1.025		328.7 1.230	324.4 1.246	337.3 1.345	340.8 1.366	336.9 1.290	336.1 1.393	Regulating Blade	338.4 1.229	276.7 0.883
	213.9 0.599	269.7 0.856	Blade 1	313.7 1.101	309.2 1.107	319.3 1.223	322.8 1.233	317.9 1.155	323.7 1.254		303.1 1.031	237.2 0.723
7	195.4 0.512	233.2 0.709		285.5 0.897	280.3 0.959			286.4 1.006	290.8 1.038		279.5 0.864	220.2 0.618
	184.8 0.482	209.9 0.627		252.8 0.793	251.6 0.911			259.0 0.955	263.2 0.923		241.1 0.774	199.2 0.587

Key
IFE Temp
Rod PPF

Power Peaking Factors
< 0.5
0.5-0.75
0.75-1.0
1.0-1.25
1.25-1.5
> 1.5

Figure 28, Bundle 62 Center Measured IFE Temperature Distribution at 1.0MW

	B			C		D		E			F	
3	188.4 0.475	220.6 0.621		256.4 0.781	248.6 0.878			257.2 0.877	253.0 0.792		242.7 0.655	207.4 0.536
	181.2 0.504	215.9 0.704		254.4 0.879	242.8 0.932			262.0 0.929	258.2 0.900		243.1 0.749	196.0 0.567
4	203.1 0.599	248.0 0.854	Blade 2	291.7 1.079	278.7 1.068	302.0 1.155	305.4 1.167	281.4 1.077	283.6 1.109	Blade 3	276.8 0.916	222.3 0.678
	219.7 0.750	264.9 1.035		310.1 1.211	302.6 1.217	309.1 1.309	318.9 1.449	304.5 1.256	302.6 1.258		287.7 1.130	236.8 0.849
5				313.6 1.278	311.6 1.306	1.566		341.4 1.491	310.3 1.352			
				315.2 1.286	315.4 1.312	1.435	1.581	327.2 1.369	315.4 1.391			
6	237.7 0.741	286.7 1.025		308.9 1.230	305.5 1.246	315.4 1.345	319.8 1.366	315.9 1.290	312.6 1.393	Regulating Blade	320.2 1.229	266.9 0.883
	206.6 0.599	259.4 0.856	Blade 1	296.9 1.101	293.4 1.107	300.5 1.223	304.3 1.233	298.1 1.155	303.2 1.254		283.3 1.031	226.3 0.723
7	190.4 0.512	227.6 0.709		274.4 0.897	266.5 0.959			269.8 1.006	275.4 1.038		264.4 0.864	210.6 0.618
	181.4 0.482	205.3 0.627		242.2 0.793	240.3 0.911			243.6 0.955	251.2 0.923		229.2 0.774	192.4 0.587

Key
IFE Temp
Rod PPF

Power Peaking Factors
< 0.5
0.5-0.75
0.75-1.0
1.0-1.25
1.25-1.5
> 1.5

Figure 29, Bundle 62 Bottom Measured IFE Temperature Distribution at 1.0 MW

The graph of center thermocouple temperature vs. pin power peaking factor is shown below, with the expected linear fit.

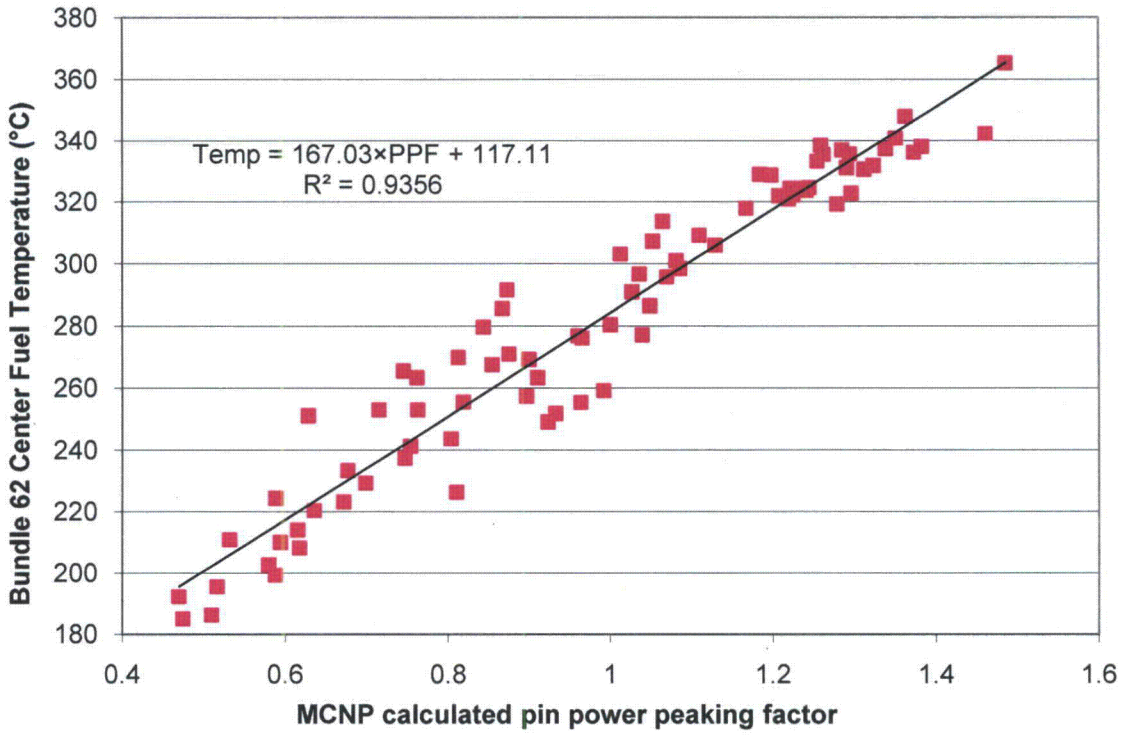

Figure 30, Bundle 62 Center Fuel Temperature vs. Pin PPF

During measurements, a typical variability of 1 °C was observed during a single full power run, while the variability in the same location during multiple full power runs was as much as 5 °C. Furthermore, in two locations the IFE was rotated to see how the observed temperature varied with thermocouple direction. One location was near the center of the core where the flux gradient is relatively flat, and rotating the IFE varied the temperature by less than 5 °C. The second location was on the periphery of the core where the flux gradient is large, and rotating the IFE varied the temperature by as much as 15 °C. In addition to the variability in IFE thermocouple readings, the pin power peaking factors were calculated using MCNP for the entire pin, rather than the local power being produced at the thermocouple location which also accounts for some of the scatter observed in Figure 30.

For the five locations in which both IFEs were measured, the IFE in bundle 72 measured higher than the IFE in bundle 62 by 68 °C on average, with a scatter of ± 17 °C. See Table 22. It is likely that this discrepancy is due to differences in fuel swelling and contact with the thermocouples within each IFE. It is also possible that the difference in measured temperatures was due to unequal burnup and samarium buildup between IFE bundles. The critical bank height during temperature mapping ranged from 12.30 to 12.69 inches as fuel was shuffled, even when

there was no xenon in the core. Although the temperature mapping was an attempt at measuring BOL conditions, there was a total of 68.87 MWh of core exposure when temperature mapping began due to previous power calibrations and other required operations, including steady-state operation to verify no trending in IFE temperatures.

Table 23, Predicted vs. Measured IFE Temperatures

	LEU Predicted	LEU Measured	
		Bundle 62	Bundle 72
D4 SW Temp (°C)	391-480	342.3	405.3
E3 NE Temp (°C)	264-317	269.1	318.6

J. FLUX MEASUREMENTS

The neutron flux was measured in most of the irradiation facilities and in the core using neutron activation of samples. For the experimental facilities, multiple irradiations of gold, gold wrapped in cadmium, and nickel were used to calculate thermal, epithermal, and fast neutron flux. The results are given below.

Table 24, Experimental Facility Flux Measurements

		LEU Measured [n/cm^2/sec]
Whale C2	Thermal	8.73×10^{12}
	Epithermal	6.93×10^{11}
	Fast	2.74×10^{12}
Whale C8	Thermal	1.20×10^{13}
	Epithermal	6.10×10^{11}
	Fast	2.68×10^{12}
Whale E8	Thermal	1.72×10^{13}
	Epithermal	4.52×10^{11}
	Fast	2.89×10^{12}
Pneumatic Tube	Thermal	4.45×10^{12}
	Epithermal	1.34×10^{11}
	Fast	7.28×10^{11}
Thermal Column	Thermal	1.70×10^{8}

For the in-core axial flux profile, it was desired to use a miniature fission chamber probe which could be raised and lowered inside a fuel coolant channel while at full power, but the probe failed and could not be readily repaired. Instead of using the miniature fission chamber, a gold wire attached to an aluminum rod was activated in the coolant channel following the UWNR 002 procedure. The procedure limits maximum reactor power to 1kW. The rod was positioned between D5 and D6, the hottest available position. After irradiation, the gold wire was cut into ½ inch long segments and counted individually in order to construct the axial flux profile, shown in Figure 31. During measurement, the control elements were at a bank height of 10.42 inches compared to the full power bank height of 12.58 inches.

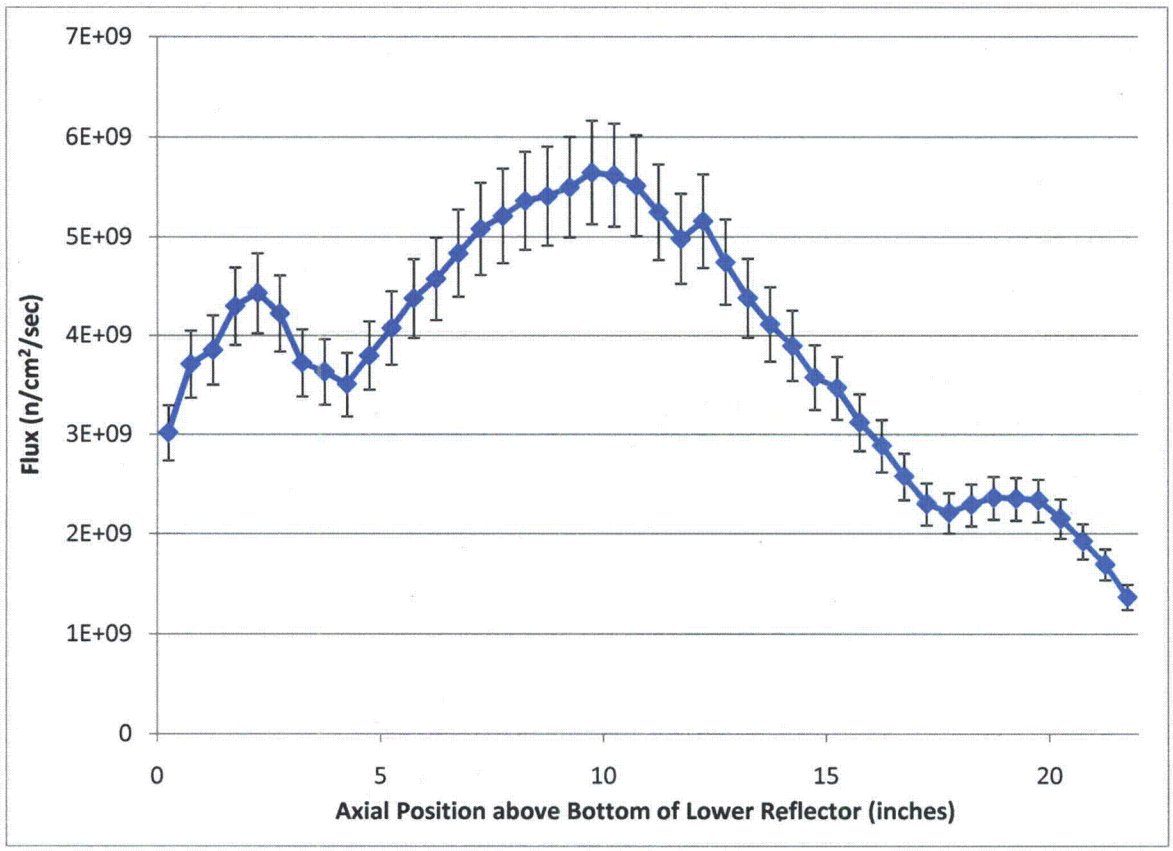

Figure 31, LEU Axial Flux Profile

K. PULSE TESTING

Pulse testing began after 79.73 MWh of core exposure. Pulses ranged from the minimum operationally allowed 1.000 %Δk/k to the maximum achieved of 1.363 %Δk/k insertion. LEU measured pulse data is shown in Table 25. Figure 32 shows peak fuel temperature vs. reactivity insertion, Figure 33 shows integrated pulse power (energy) vs. reactivity insertion, and Figure 34 shows peak power vs. the square of reactivity insertion. All graphs show the expected linear trend, except for some of the larger pulses which may deviate from linearity due to slow transient rod ejection times with respect to pulse width. The graph of fuel temperature shows that the first 1.2 %Δk/k pulse data point is well above the linear fit, therefore this point was re-taken with a much better result. The initial outlier point is assumed to be attributed to electrical noise which was not reproducible.

During pulse testing, no increased stack or continuous air monitor readings were detected, and routine air and pool water samples continue to indicate no fission product release.

Table 25, LEU Pulse Data

Reactivity Insertion (%Δk/k)	Peak Power (MW)	Peak Fuel Temperature (°C)	Integrated Pulse Power (MJ)	FWHM (ms)	Period (ms)
1.000	80.26	186	2.77	39.30	9.81
1.026	89.72	185	3.35	36.17	8.16
1.050	144.75	193	4.21	29.03	7.81
1.075	159.99	197	4.52	26.12	6.71
1.100	206.89	206	5.32	22.83	5.66
1.125	229.06	206	5.55	21.56	5.60
1.150	280.87	217	6.28	19.87	5.19
1.150	281.93	216	6.19	19.77	5.22
1.175	306.98	217	6.36	18.91	4.32
1.200	361.59	277	7.24	17.55	3.52
1.200	345.87	221	6.96	17.42	4.63
1.225	385.26	227	7.39	17.05	3.96
1.250	435.92	236	7.97	16.20	4.23
1.275	470.85	235	8.35	15.49	4.04
1.300	496.00	239	8.63	15.28	4.01
1.325	551.42	243	9.03	14.54	4.51
1.350	589.16	251	9.58	14.30	3.81
1.363	594.41	251	9.67	14.24	3.36
1.363	595.16	250	9.59	14.25	3.83

The LEU peak powers are noticeably smaller than for the previous HEU core, which can be explained by the reduced total core heat capacity due to the reduction in fuel pins.

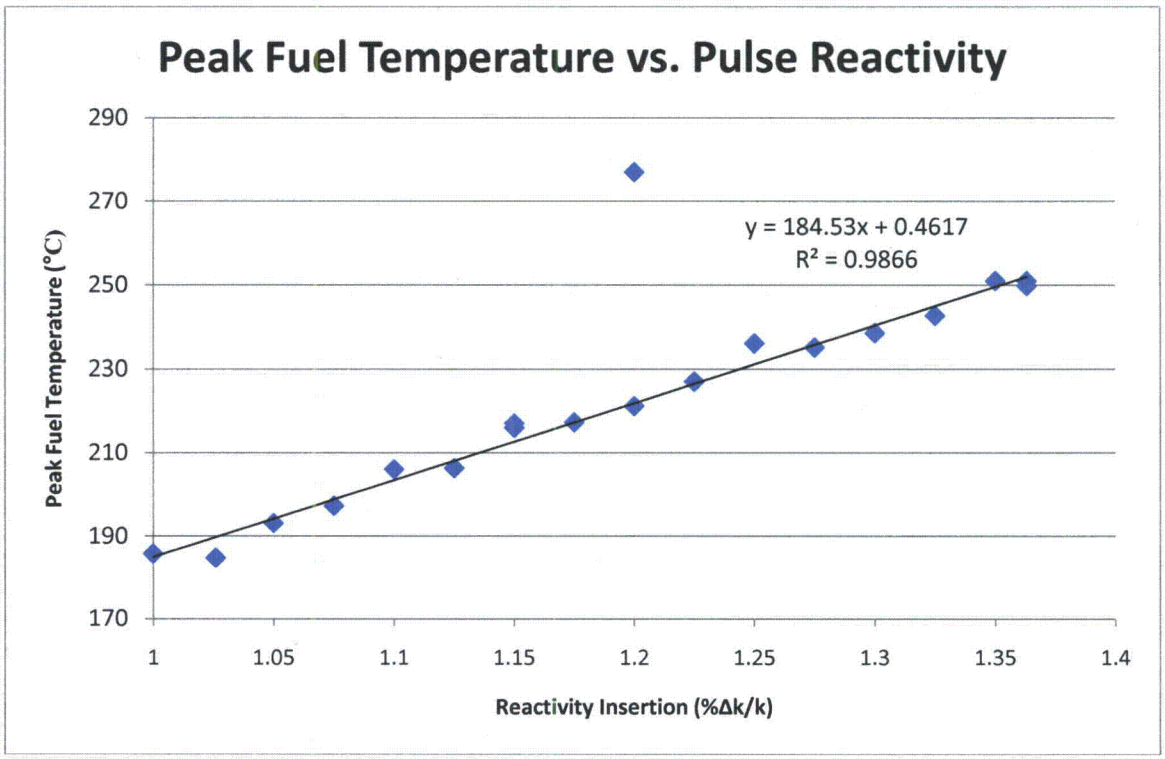

Figure 32, Peak Fuel Temperature vs. Pulse Reactivity

The linear fit equation shown in Figure 32 was made after excluding the outlier point at 1.2 %Δk/k.

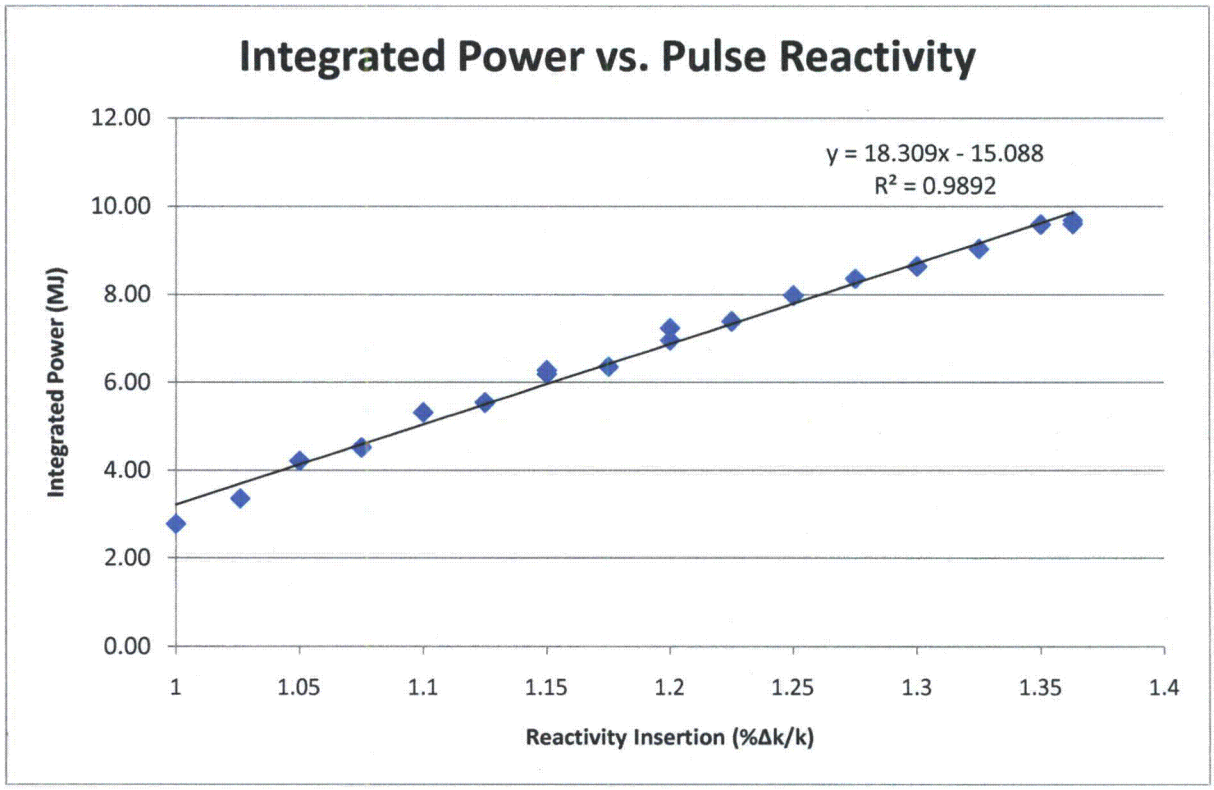

Figure 33, Integrated Power vs. Pulse Reactivity

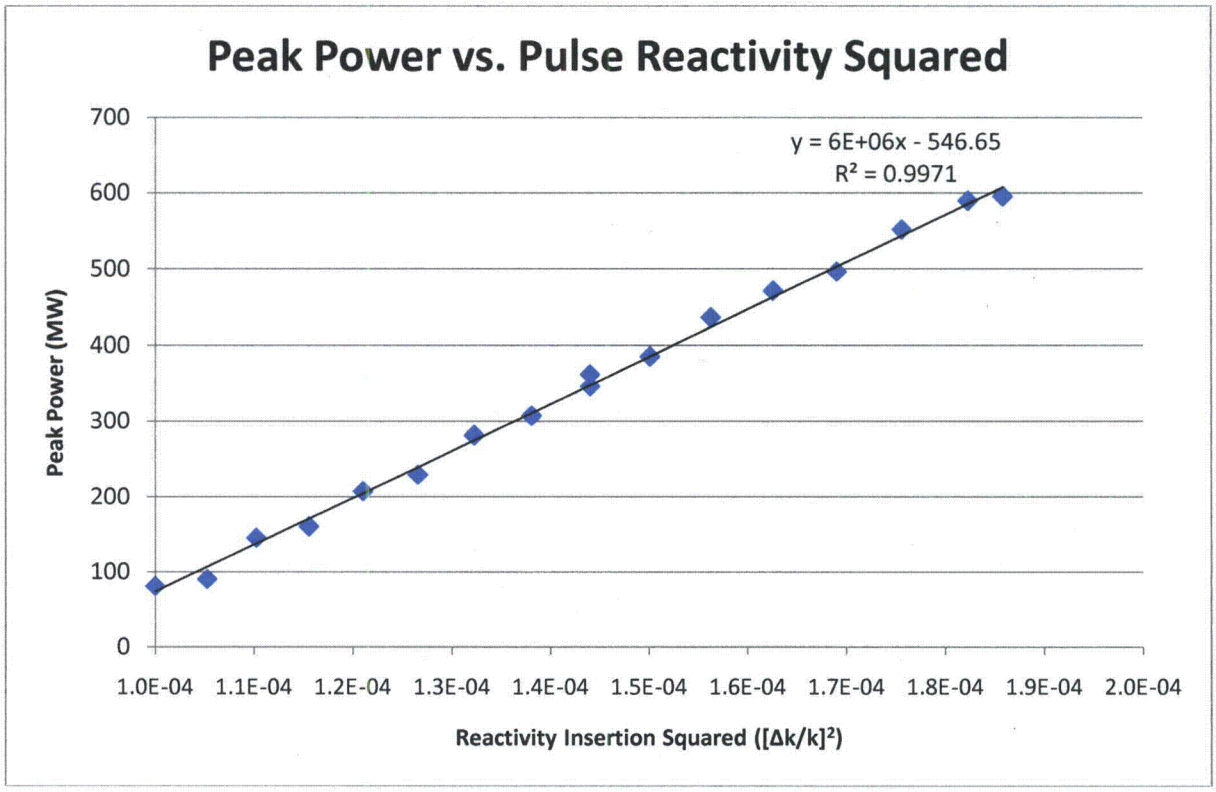

Figure 34, Peak Power vs. Pulse Reactivity Squared

The value of β, ℓ_p, and α can be estimated from the measured data using several methods. First, from reactor kinetics the following equation relates β and ℓ_p to the measured period.

$$\tau = \frac{\ell_p}{\rho - \beta}$$

or

$$\omega = \frac{1}{\tau} = \frac{\rho - \beta}{\ell_p}$$

Where: τ = period [ms]
ρ = pulse reactivity insertion [$\Delta k/k$]
β = delayed neutron fraction
ℓ_p = prompt neutron lifetime [ms]
ω = inverse period [ms^{-1}]

Therefore, by plotting the inverse period vs. reactivity insertion the slope of the line is the inverse of the prompt neutron lifetime and the y-intercept is related to the delayed neutron fraction. This is shown in Figure 35 where the R^2 value is 0.82, and the calculated values of ℓ_p = 22.2μs and β = 0.0072.

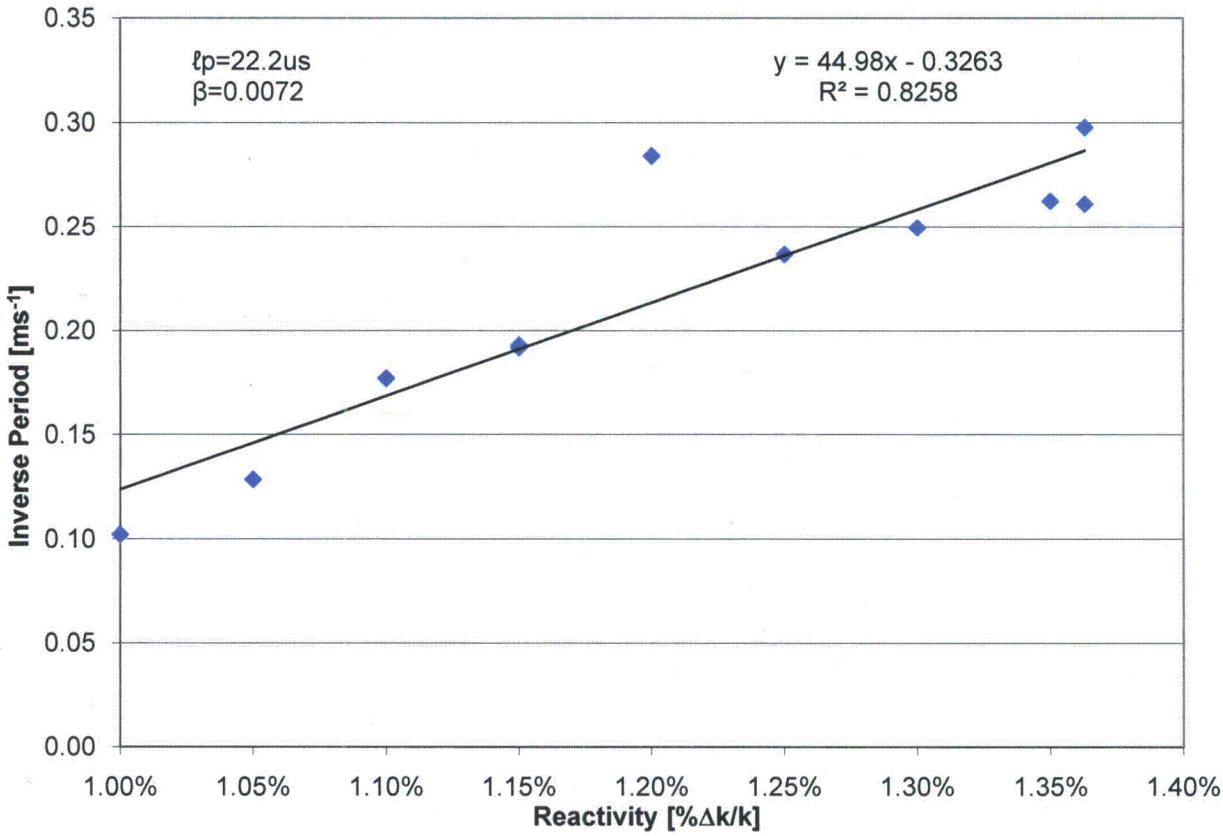

Figure 35, Inverse Period vs. Reactivity

Alternatively, by applying the Fuchs Nordheim model for reactivity feedback the pulse full width at half maximum (FWHM) is related to the reactivity insertion according to the following equation. This is shown in Figure 35 where the R^2 value is 0.97, and the calculated values of $\ell_p = 24.4\mu s$ and $\beta = 0.0074$.

$$\frac{1}{\Omega} = \frac{\rho}{4\cosh^{-1}\sqrt{2}\ell_p} - \frac{\beta}{4\cosh^{-1}\sqrt{2}\ell_p}$$

Where: ρ = pulse reactivity insertion [Δk/k]
β = delayed neutron fraction
ℓ_p = prompt neutron lifetime [ms]
Ω = FWHM [ms]

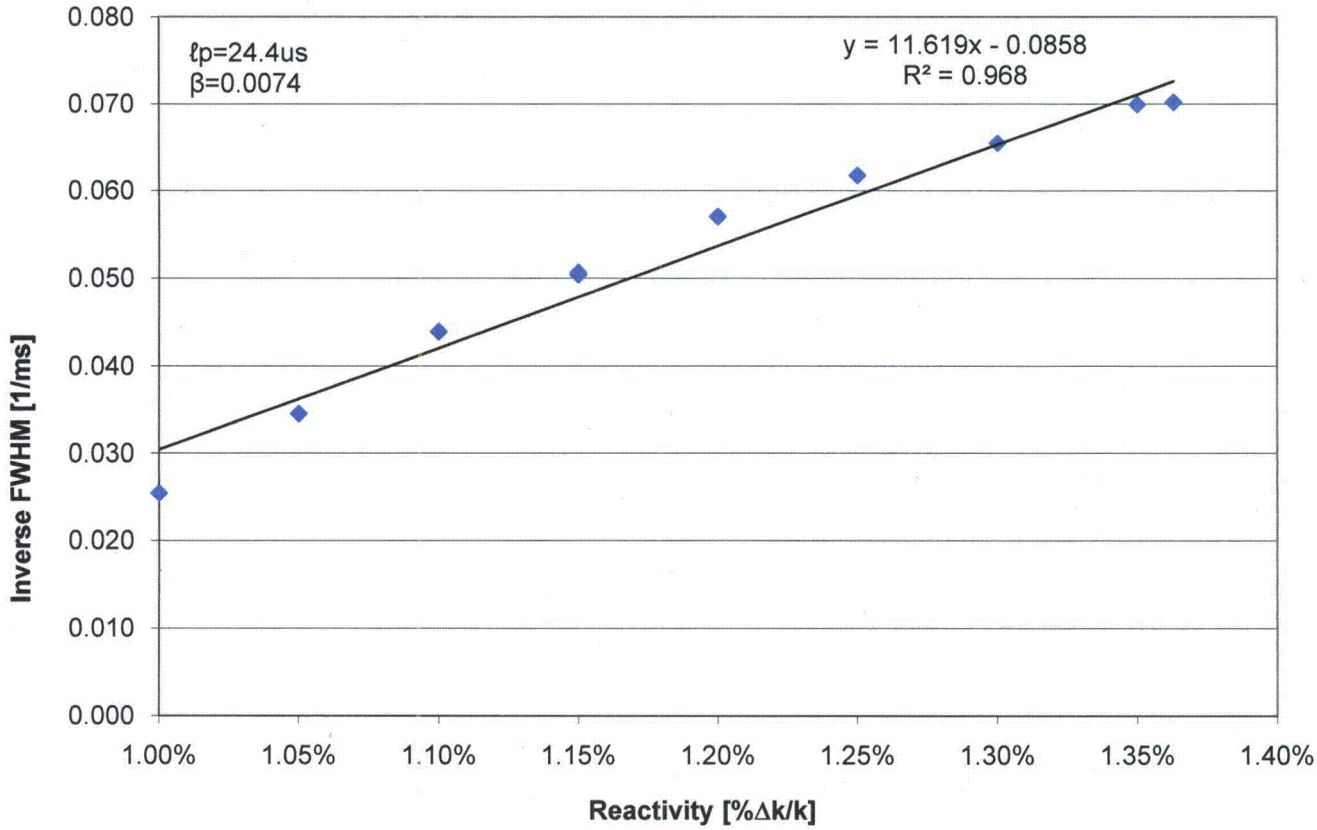

Figure 40, Inverse Full Width at Half Maximum vs Reactivity Insertion

The values of β and ℓ_p, as determined both from reactor kinetics and the Fuchs Nordheim model, were averaged and summarized below in Table 26.

Table 26, Predicted vs. Measured β and ℓ_p

	LEU Predicted	LEU Measured
Delayed neutron fraction β	0.0078	0.0073
Prompt neutron lifetime ℓ_p	27.1μsec	23.3μsec

L. SQUARE-WAVE TESTING

Performing a square-wave operation involves firing the transient rod while at low power to insert a large amount of reactivity, but less than beta, to allow the power to quickly rise to its peak value, then withdrawing control elements in order to maintain the power level. Before performing a square-wave, the relation of peak power vs. transient rod height must first be measured to allow square-waving to the desired power. This is done by firing the transient rod at a variety of heights and observing the peak power achieved, without withdrawing any control elements. Therefore power is allowed to decrease after reaching the peak and then the reactor is shutdown. The data is in the table below, followed by the square-wave curve to be used for future square-wave operations.

Table 27, Square-wave Data

T-rod Height (inches)	Peak Power (kW)
10.65	66
10.90	110
11.25	222
11.75	556
11.95	840
12.03	962
12.05	971

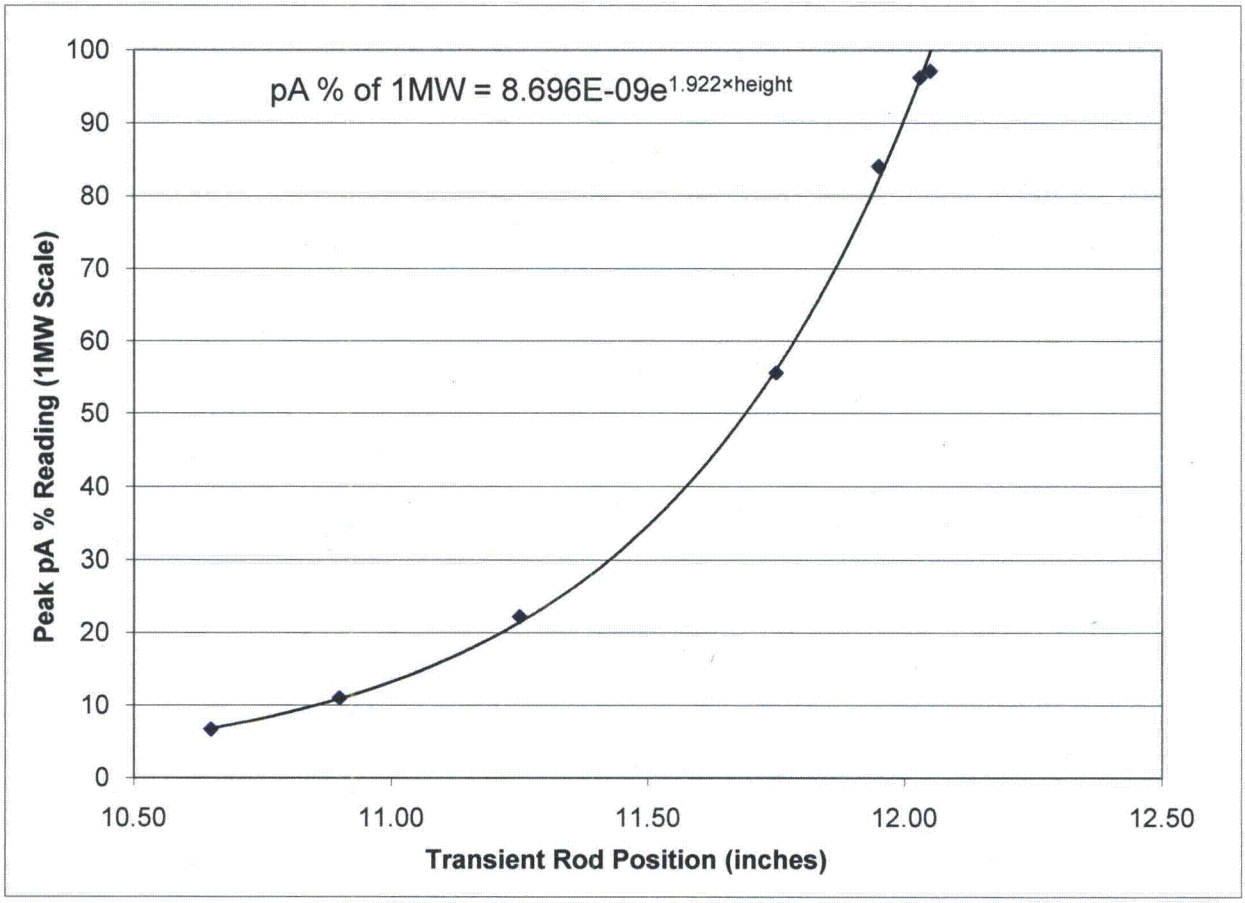

Figure 36, Square-wave Curve

M. SUMMARY OF HEU MEASUREMENTS VS. LEU PREDICTIONS AND MEASUREMENTS

Table 28 is a summary of all predicted vs. measured values reported earlier in this report. Comparisons are also made to measured values on the HEU core, where available. Fluxes are compared in Table 29 and Table 30.

Table 28, Predicted vs. Measured Values

	HEU Measured	LEU Predicted	LEU Measured
Critical bundles	18	19	18
Cold critical bank height [inches]	9.50	10.13	10.24
Void coefficient [%Δk/k per %void]	-0.2	-0.149	-0.14
Flooding pn tube [%Δk/k]	+0.0002	+0.007	+0.004
B_4C in pn tube [%Δk/k]	N/A	N/A	-0.007
Cd in pn tube [%Δk/k]	-0.0005	-0.009	-0.009
Air whale in E8 [%Δk/k]	N/A	N/A	-0.030
Graphite whale in E8 [%Δk/k]	N/A	N/A	+0.011
Lead whale in E8 [%Δk/k]	N/A	N/A	+0.003
Cd whale in E8 [%Δk/k]	N/A	-0.04	-0.087
Hot critical bank height [inches]	11.50	11.73	12.58
Power coefficient [%Δk/k/kW]	N/A	N/A	-1.22E-3
Fuel temperature coefficient [%Δk/k/°C]	-1.26E-2	-4.08E-3 (300-400K) -6.58E-3 (400-600K)	-5.55E-3
D4 SW Temp [°C]	405 (Bundle 41) 492 (Bundle 42)	391-480	342.3 (Bundle 62) 405.3 (Bundle 72)
E3 NE Temp [°C]	277 (Bundle 41) 375 (Bundle 42)	264-317	269.1 (Bundle 62) 318.6 (Bundle 72)
Delayed neutron fraction β	0.0070	0.0078	0.0073
Prompt neutron lifetime ℓ_p	22μsec	27.1μsec	23.3μsec

Table 29, Flux Comparison HEU vs. LEU

		HEU Measured	LEU Measured
Whale C2	Thermal	8.80×10^{12}	8.73×10^{12}
	Epithermal	2.65×10^{11}	6.93×10^{11}
	Fast	2.12×10^{12}	2.74×10^{12}
Whale C8	Thermal	7.55×10^{12}	1.20×10^{13}
	Epithermal	3.11×10^{11}	6.10×10^{11}
	Fast	2.34×10^{12}	2.68×10^{12}
Whale E8	Thermal	8.06×10^{12}	1.72×10^{13}
	Epithermal	3.59×10^{11}	4.52×10^{11}
	Fast	2.68×10^{12}	2.89×10^{12}
Pneumatic Tube	Thermal	3.32×10^{12}	4.45×10^{12}
	Epithermal	1.23×10^{11}	1.34×10^{11}
	Fast	5.64×10^{11}	7.28×10^{11}
Thermal Column	Thermal	1.65×10^{08}	1.70×10^{8}

The LEU Conversion SAR estimated the change in flux by calculating the ratio of LEU flux to HEU flux values (where the flux used was total neutron flux in the entire energy range). To compute this ratio, the sum of thermal, epithermal, and fast fluxes were compared.

Table 30, Predicted vs. Measured Experimental Facility Fluxes

	LEU Predicted	LEU Measured
Flux ratio LEU/HEU Whale C2	1.27	1.09
Flux ratio LEU/HEU Whale C8	1.26	1.50
Flux ratio LEU/HEU Whale E8	1.25	1.85
Flux ratio LEU/HEU Thermal Column	1.05	1.03

The LEU measured axial flux profile is shown again in Figure 37 compared to the HEU measured flux profile. Note that the HEU measurement was in relative units of probe current and not flux, but the HEU axial profile was arbitrarily adjusted in the vertical axis in order to overlay the LEU measurement to make a comparison of the shape.

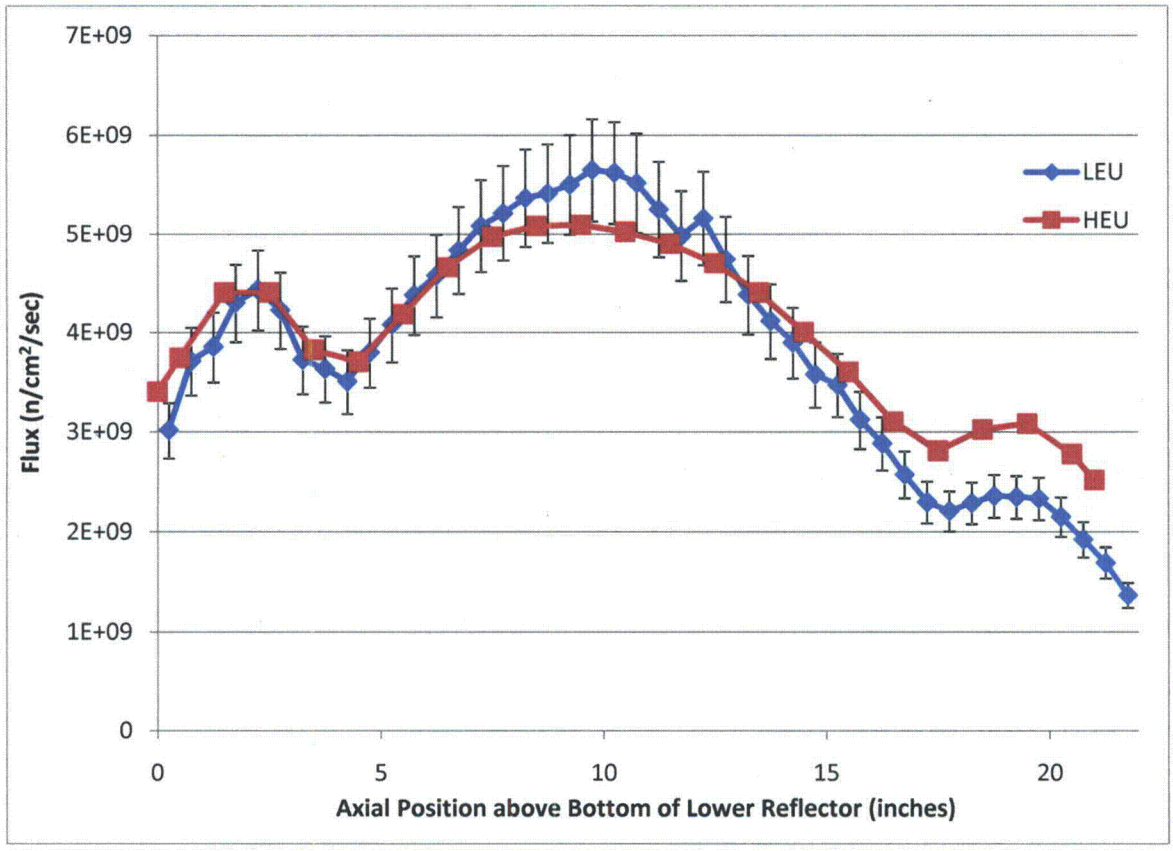

Figure 37, Axial Flux Comparison HEU vs. LEU

Table 31 shows a comparison of pulsing values for the HEU and LEU cores. The number of HEU pulses was more limited so not all LEU pulses from Table 25 were compared.

Table 31, Pulse Comparison HEU vs. LEU

	Reactivity Insertion (%Δk/k)	Peak Power (MW)	Peak Fuel Temperature (°C)	Integrated Pulse Power (MJ)	FWHM (ms)	Period (ms)
HEU	1.000	111	198	2.64	39.42	10.58
LEU	1.000	80.26	186	2.77	39.30	9.81
HEU	1.050	178	207	3.55	29.24	8.09
LEU	1.050	144.75	193	4.21	29.03	7.81
HEU	1.100	284	216	5.02	22.26	6.22
LEU	1.100	206.89	206	5.32	22.83	5.66
HEU	1.150	383	228	5.91	19.09	5.43
LEU	1.150	281.93	216	6.19	19.77	5.22
HEU	1.200	506	233	6.53	16.59	4.79
LEU	1.200	345.87	221	6.96	17.42	4.63
HEU	1.250	629	241	8.25	14.80	4.36
LEU	1.250	435.92	236	7.97	16.20	4.23
HEU	1.300	746	252	8.38	13.60	4.10
LEU	1.300	496.00	239	8.63	15.28	4.01
HEU	1.350	863	262	9.45	12.70	3.91
LEU	1.350	589.16	251	9.58	14.30	3.81

N. COMPUTING MCNP MODEL BIAS

In addition to the cold and hot bank height measurements noted above, a number of cold critical control element configurations were measured and added to the already existing rod calibration and reflector reactivity database in order to establish the criticality bias of the MCNP model of the LEU core (calculated below). In addition, the original MCNP model used for the LEU Conversion SAR used nominal fuel material definitions since the fuel had not yet been fabricated, but these fuel material definitions were updated to reflect as-built fuel data received from the manufacturer. The resulting bias in both the cold and hot models was surprisingly large. This led to an investigation of the MCNP model and possible sources of inaccuracies leading to the large bias. Several changes were made to the model as a result, summarized below:

- Transient rod was incorrectly defined as 1.25in diameter for the poison section, instead of the correct value of 1.25in diameter for the outside clad, and the fairly large bottom fitting had been neglected in the model; the fitting was added to correctly account for the displacement of water volume. Also the density of the poison section was slightly modified based on as-built documentation from the manufacturer.
- Shim safety blades were incorrectly defined as 3/8in thick boral with 1/8in clad, instead of the correct value of 1/8in thick boral with 1/8in clad for 3/8in total thickness. Also the rounded corners of the blades were added into the model.
- Reflector dimensions were updated using as-built drawings of the newly fabricated reflectors. Also, a small boron impurity was added to the graphite based on a material analysis report from the reflector manufacturer indicating level of equivalent boron content.
- A small boron impurity of 10ppm was added to the aluminum material definition. This is a typical value used in research reactor modeling when no aluminum material analysis is available.
- Graphite density in the axial reflectors within fuel pins was reduced or "smeared" to account for the smaller diameter of graphite slugs compared to fuel slugs.
- Cross-section libraries for uranium isotopes were switched to UTXS libraries to be consistent with erbium isotopes.
- A small hafnium impurity was added to the zirconium pin material consistent with the Hf/Zr ratio present in the fuel.
- Water density in the hot model core was reduced to the equivalent of a water temperature of 50°C (instead of 30°C); 50°C is the approximate core averaged water temperature at 1.0MW.

Prior to changing the transient rod and shim safety blades in the model, the measured bias had a large degree of scatter and showed some trends when plotted vs. control element heights; after implementing the changes the bias was very consistent with little scatter, indicating that the control elements were being accurately modeled. See Figure 38 through Figure 42.

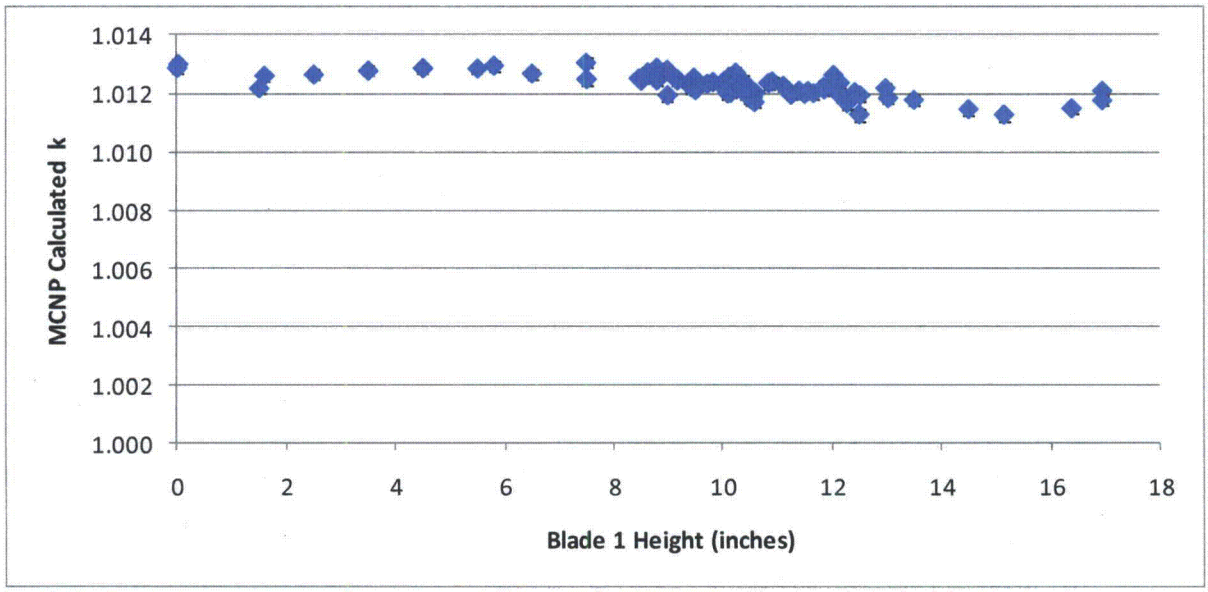

Figure 38, Calculated k vs. Blade 1 Height

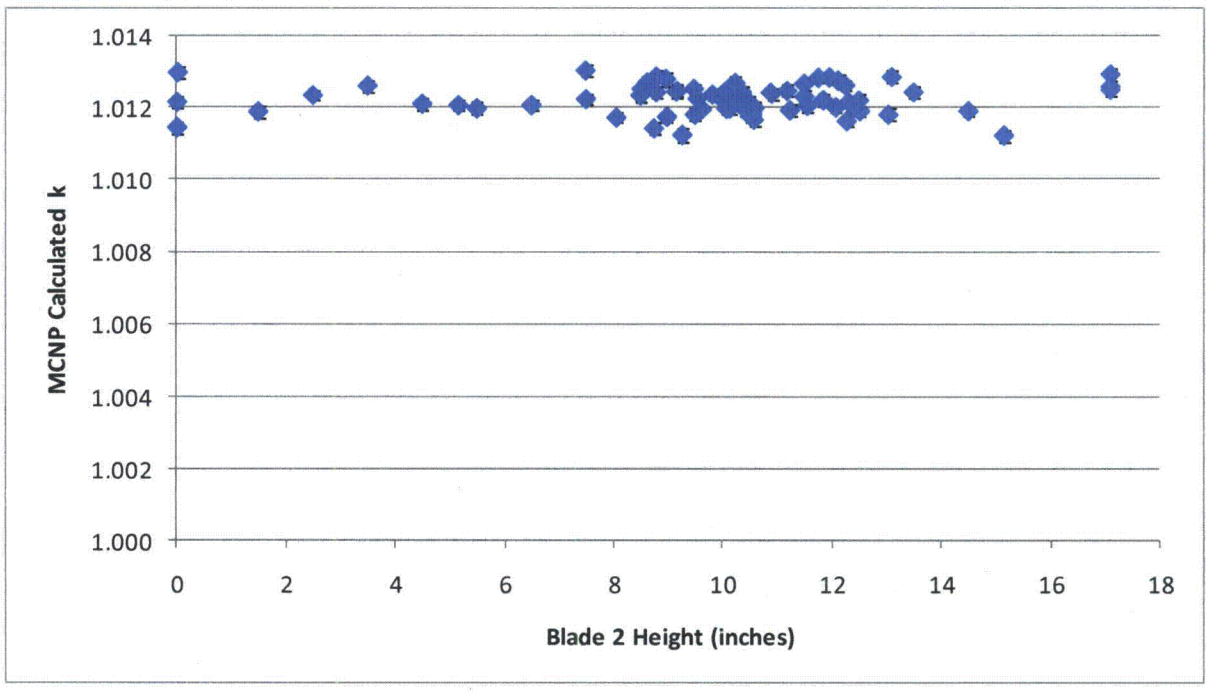

Figure 39, Calculated k vs. Blade 2 Height

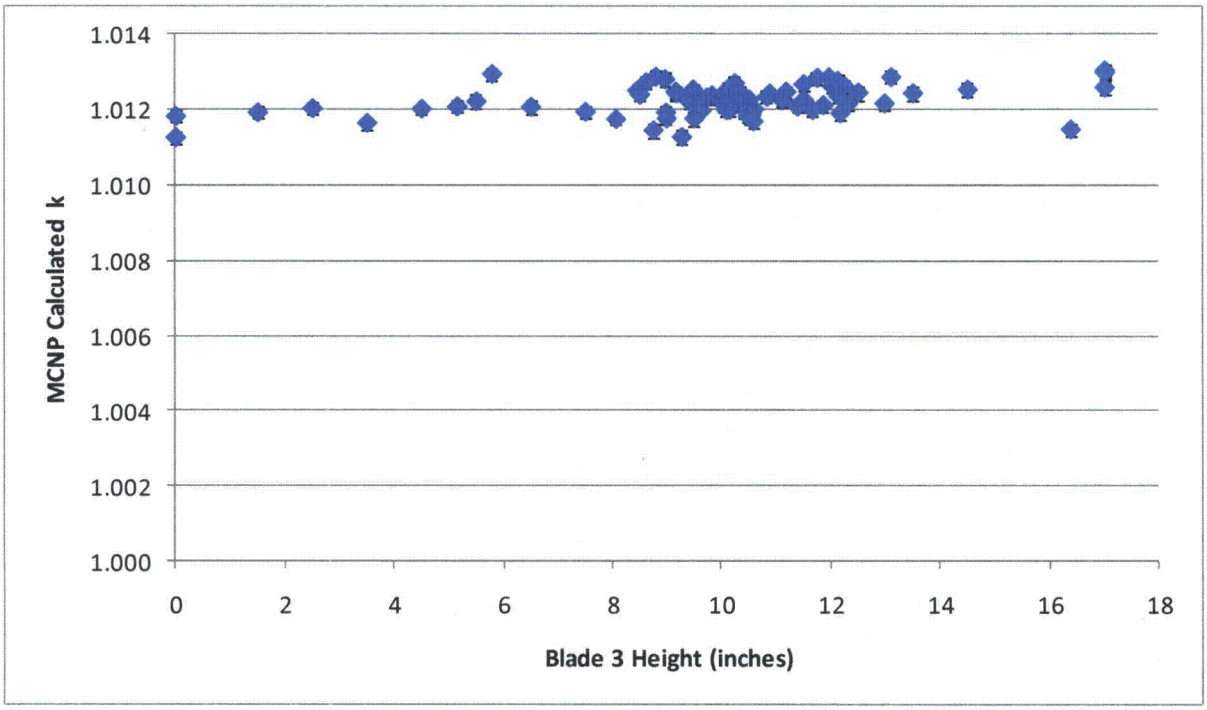

Figure 40, Calculated k vs. Blade 3 Height

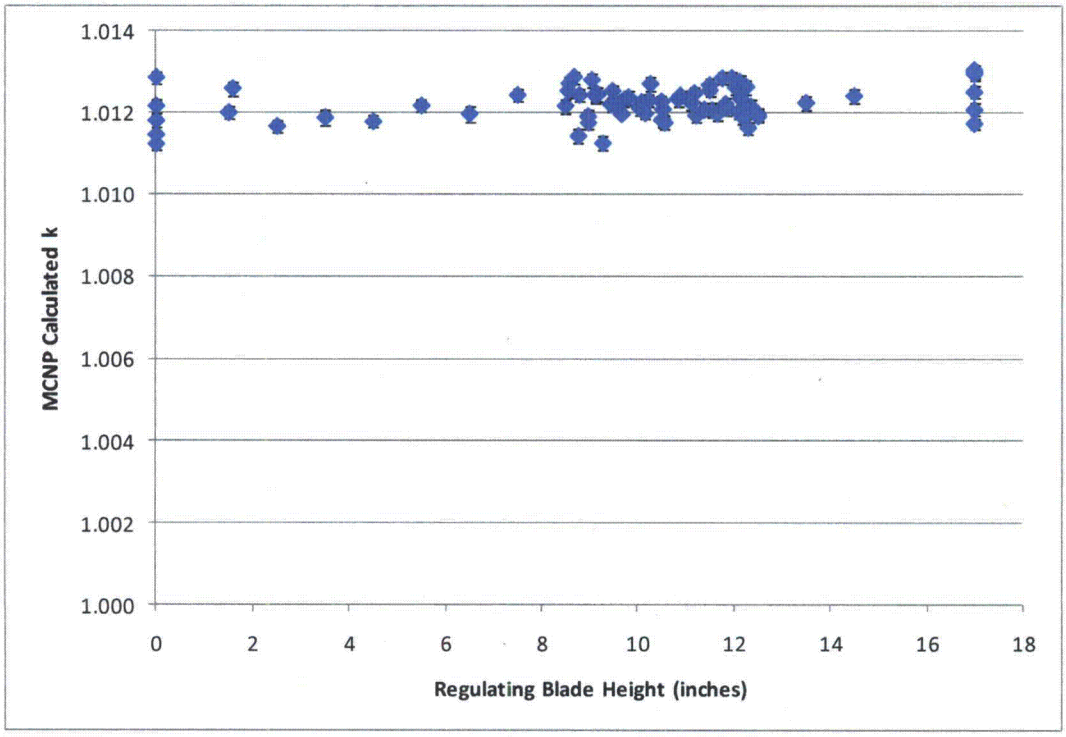

Figure 41, Calculated k vs. Regulating Blade Height

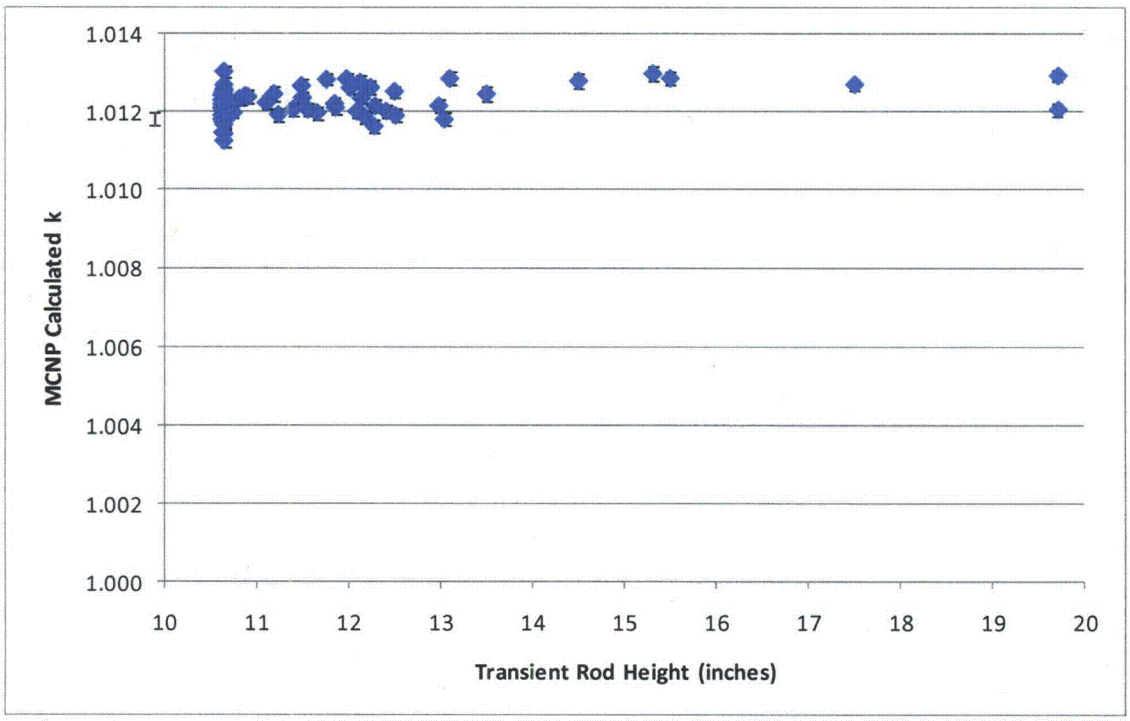

Figure 42, Calculated k vs. Transient Rod Height

By using all available cold critical configurations for the operational core J21-R14, the average k bias is 1.01222 ± 0.00040. The hot bias can only be calculated from the single full power data point as 1.00971 ± 0.00040, since operational practice is to maintain control elements banked while at power. Therefore the cold bias is 1.01222 and the hot bias is 1.00971.

The following figure shows the change in bias as fuel and reflectors are added to the core.

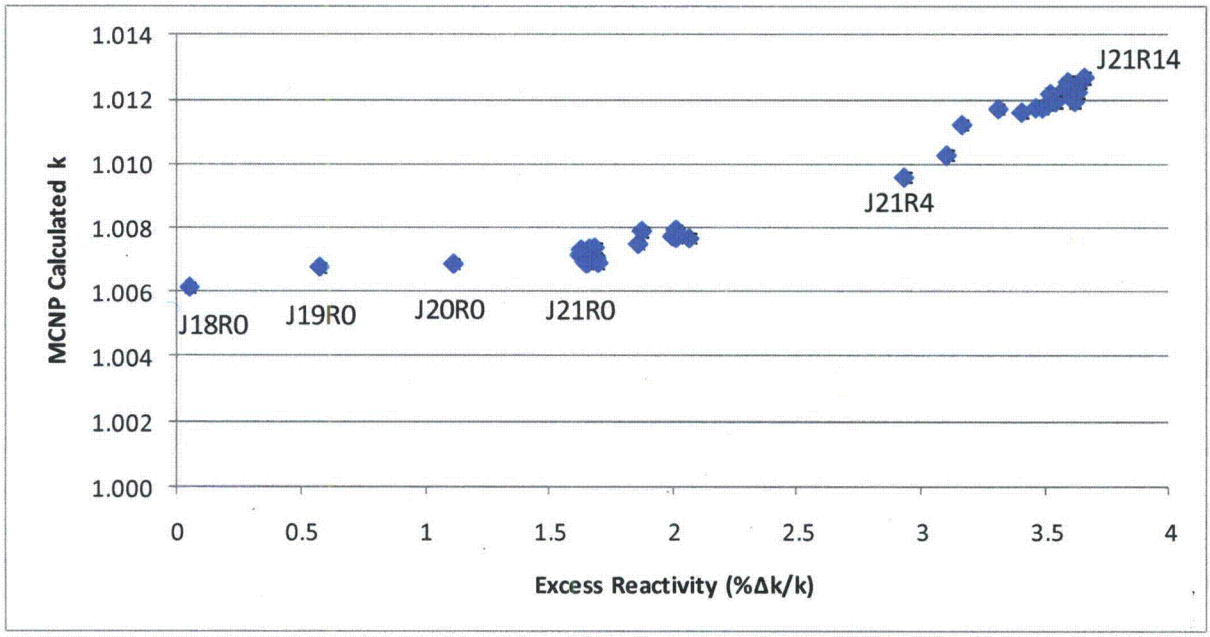

Figure 43, Calculated k vs. Core Loading

As the figure above shows, there is little change in bias as fuel is loaded indicating an accurate modeling of the fuel pins. However, there is a large jump in bias as reflectors are loaded, increasing linearly with reactivity insertion. Clearly the reflectors are being modeled as more reactive than they physically are, and this alone accounts for about half of the cold model bias. This conclusion was confirmed by review from staff at Argonne National Laboratory. However, because no reasonable solution could be found to reduce the bias in the cold or hot MCNP models, and because of the excellent consistency of cold model results, the investigation into the model bias was closed.

Using the updated MCNP model dated 2/9/2010, and implementing the known model bias, the burnup curve for the J21-R14 core was re-calculated. As seen in Figure 44, the revised curve predicts a much shorter core life. According to the LEU Conversion SAR, an operational core should have at least 0.5 %Δk/k hot excess reactivity to permit continued operation with high-worth experiments installed. The original burnup curve in the LEU Conversion SAR predicted continued operation up to 1800 MWd before falling below 0.5 %Δk/k hot excess reactivity, whereas the revised burnup curve predicts operation only until 50 MWd. Based on the revised MCNP model and well established bias, and revised burnup calculations, it is now apparent that a core reshuffle or fuel addition will be required at some point in the near future to extend core life. The analysis for this core shuffle is currently underway and will be performed as a 10 CFR 50.59 analysis or, if required, a license amendment to be submitted at a later date.

Preliminary analysis favors shuffling to a compact rounded 21 bundle core with 6 reflectors. With this rounded core, preliminary designation N21-R6, the calculated burnup curve predicts adequate operation up to 1700 MWd. Figure 44 compares the original predicted burnup curves for the HEU core and LEU core, the revised burnup curve for the LEU core, and the preliminary burnup curve for the N21-R6 LEU shuffled core.

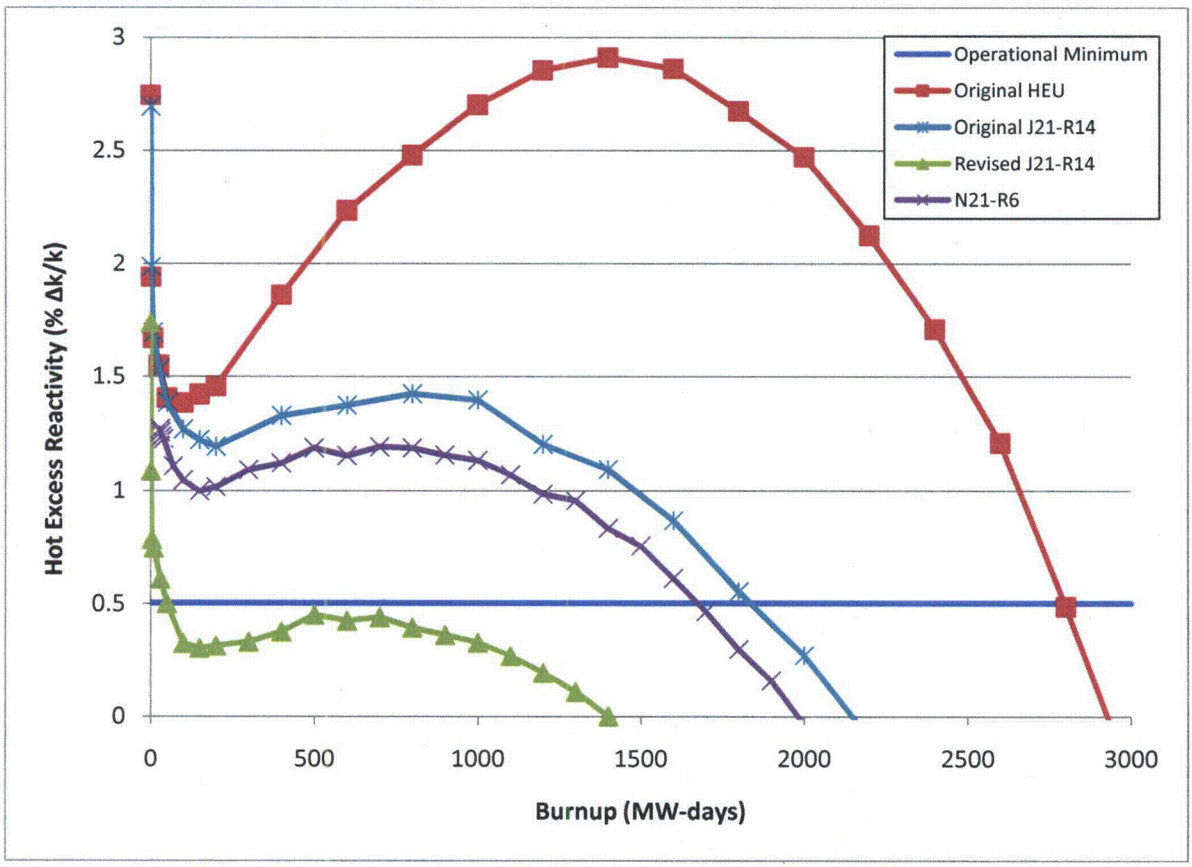

Figure 44, Burnup Curve Comparison